

Department of Environment Systems  
Graduate School of Frontier Sciences  
The University of Tokyo

2018

Master's thesis

**Evaluation of ground-level ozone change on  
introducing hybrid heavy-duty vehicles**

---

Submitted February 8th, 2019

Adviser: Professor Kenichi Tonokura  
Co-Adviser: Professor Tomohiro Tasaki

Hu Mingxi

# INDEX

1 Background introduction.....	5
1.1 Japanese transition .....	6
1.2 Ozone .....	11
1.2.1 Ozone formation .....	11
1.2.2 VOC-NOx-ozone relationship .....	13
1.2.3 Effect on human health and crops .....	15
1.3 Diesel vehicle emission .....	16
1.3.1 Emission characteristic.....	16
1.3.2 Japanese diesel consumption .....	19
1.3.2 Japanese NOx emission .....	20
1.4 Hybrid vehicle .....	22
1.5 Purpose .....	23
2 Calculation methods .....	24
2.1 WRF .....	25
2.2 CMAQ .....	27

2.3 Calculation conditions .....	30
2.3.1 Period .....	30
2.3.2 Domain .....	31
2.3.3 Emission inventory .....	33
2.3.4 Scenario .....	34
3 Results and discussion .....	36
3.1 Model validation .....	36
3.1.1 Correlation .....	36
3.1.2 preciseness .....	45
3.2 Ozone concentration change .....	53
3.2.1 Spatial distribution .....	54
3.2.2 Time series .....	58
3.2.3 Ozone increase in Tokyo Bay .....	63
3.3 Mortality estimation .....	68
4 Summary .....	71
4.1 Current conclusion .....	71

4.2 Future plan.....	72
Acknowledgement .....	73
Reference .....	74

## 1 Background introduction

Recently, with the growing recognition and strict regulations on suspending particle matter emission, the atmospheric PM<sub>2.5</sub> concentrations are well control. But in the contrary, the oxidant air pollutants precursor emissions are rather hard to control, thus leading to the tropospheric ozone formation observing in both urban and suburban areas. Direct ozone emission into the atmosphere is not in significant quantities, instead it is formed from these directly released precursor pollutants, volatile organic compounds (VOCs) and oxides of nitrogen (NO<sub>x</sub>).

Many mitigation methods have been done for this environmental issue. The hybrid vehicle developed recently may be the solution to it for reducing the fuel consumption, thus reducing exhaust emission.

By adapting atmospheric transportation model, ozone concentration caused by introduction of hybrid vehicle is calculated, and the health effect is also estimated.

## 1.1 Japanese transition

As for Japanese government, several laws have been published to cope with these photochemical reaction precursors.

For NO<sub>x</sub>, *Air Pollution Control Act*, published in 1968, firstly regulated the maximum permissible limits for the quantities of automobile exhaust by the Minister of the Environment. Passed in 1992 and most amended in 2011, *Automobile NO<sub>x</sub>/PM Act* demands further reduction on emission quantities.

And for VOCs, *Law concerning Pollutant Release and Transfer Register*, published by the Ministry of Economy, Trade and Industry in 2001, legislate corporations and plants to publish the emission of chemical materials. With the latest modification in 2013, *the Air Pollution Control Act* suppress the VOCs emission from automobile vehicles.

Environmental standard for nitrogen dioxide and photochemical oxidants is legislated by the Ministry of the Environment. For nitrogen dioxide, the daily average for hourly values shall be within the 0.04-0.06 ppm zone or below. For photochemical oxidants, hourly values shall not exceed 0.06 ppm. However, for the emission of volatile organic compounds, there is no specific legislation on hourly emission. Currently used standard comes from Air Quality Guidelines (1976, July 30th), 3-hours average concentration shall be less than 0.02-0.031ppmC from 6 a.m. to 9 a.m.

Table 1.1 shows the Japanese environmental standards.

Table 1.1 Environmental standards

<b>Substance</b>	<b>Environmental conditions</b>
Nitrogen dioxide	The daily average for hourly values shall be within the 0.04-0.06 ppm zone or below that zone
Volatile Organic Compounds	Three hours average shall be less than 0.20-0.31ppmC from 6 a.m. to 9 a.m. (Air Quality Guideline)
Photochemical oxidants	Hourly values shall not exceed 0.06 ppm

Fig.1.1 shows the NO<sub>x</sub> concentration observed by air pollution monitoring station and Motor Vehicle Exhaust Monitoring Station. It shows that in both monitoring type stations, the emission of NO<sub>x</sub> decreased significantly in recently years

Fig.1.2 shows the concentration of Non-methane hydrocarbons (NMHC) from 6 a.m. to 9 a.m. It shows that the NMHC concentration also decreased simultaneously.

Fig.1.3 shows the oxidant concentration annual change. Unlike its precursor, concentrations for oxidant are quite stable, even increasing during recently years. The increase of oxidant is in association with the complicated NO<sub>x</sub>-VOC-ozone sensitivity, deeply affected by the automobile emission.

Several reasons have been concluded to explain this symphony.

The background level of tropospheric ozone is increasing, and because of the jumping increase of NO<sub>x</sub> emission, the transboundary transportation is become severe recently, this can be one of the reasons for long-term oxidant increase.

Non-methane hydrocarbon and NO<sub>x</sub> are the precursor of photochemical oxidant, the ratio between non-methane hydrocarbon and NO<sub>x</sub> also effect the ozone formation mechanism. For the area around Tokyo Metropolitan, its ratio high ratio maybe the reason for high oxidant concentration. Further introduction on VOC-NO<sub>x</sub>-ozone will be introduced in the part of ozone,

From 1990, the ultraviolet radiation is increasing as well, there is the possibility of strengthening the photochemical reaction.

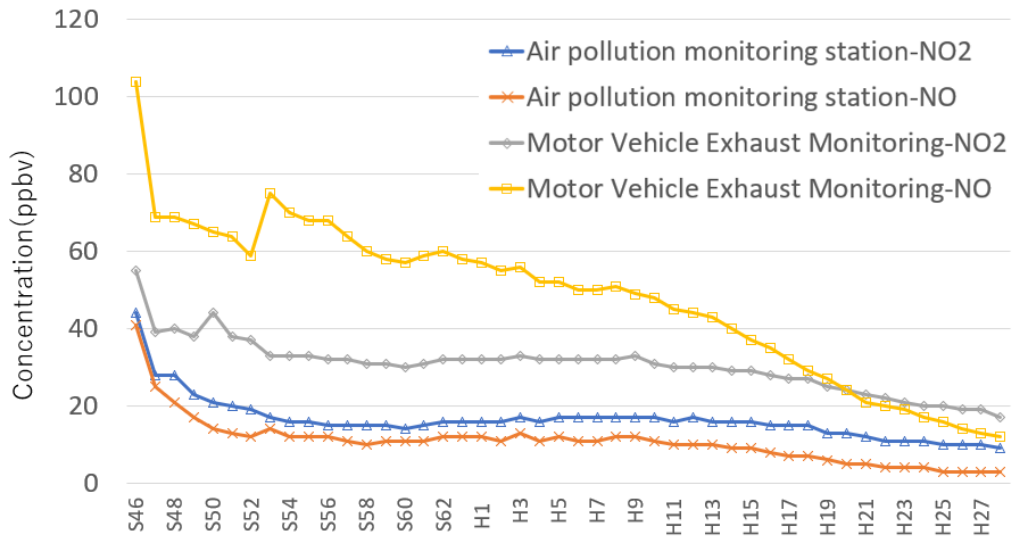


Fig.1.1 NOx concentration transition of annual average<sup>[1]</sup>

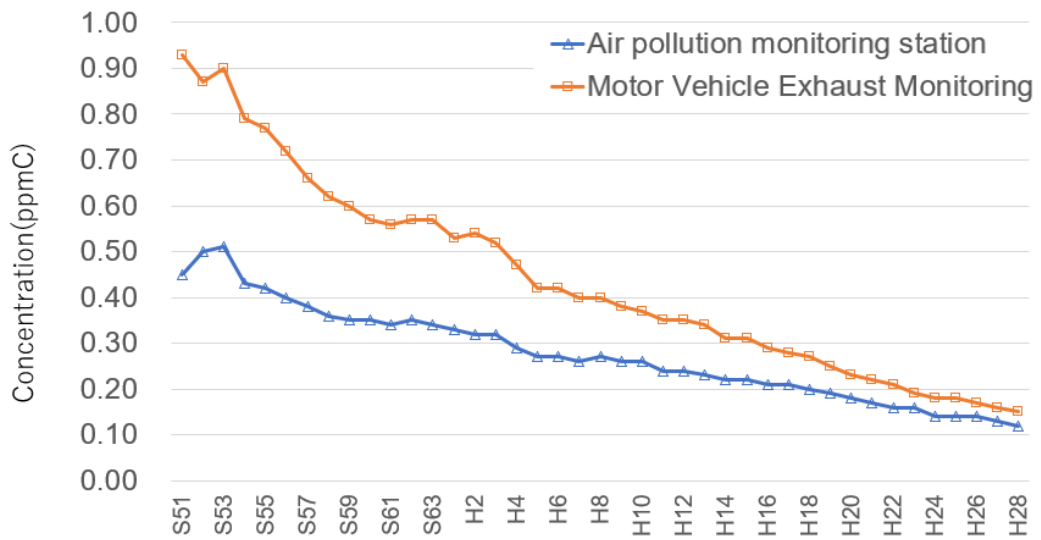


Fig.1.2 NMHC concentration transition of annual average<sup>[1]</sup>

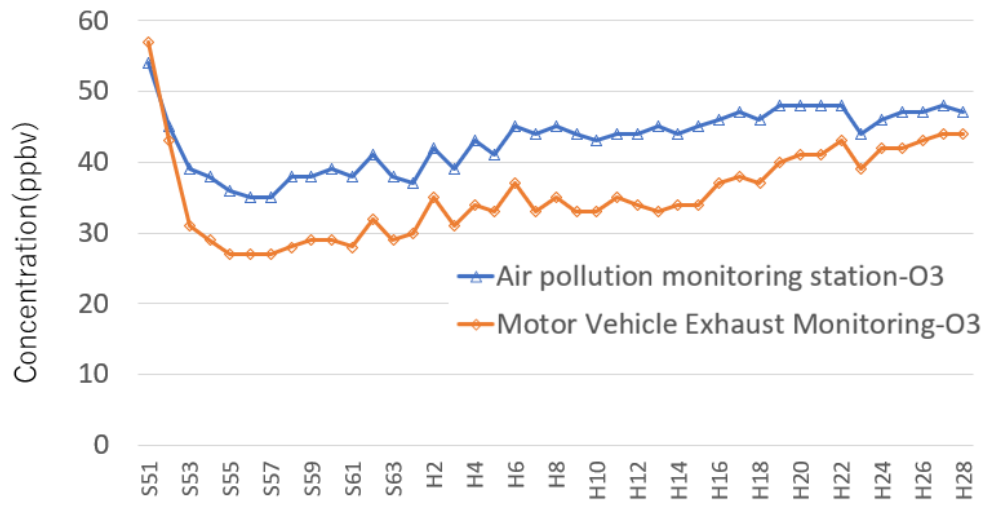


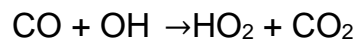
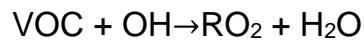
Fig.1.3 Oxidant concentration transition of annual average<sup>[1]</sup>

## 1.2 Ozone

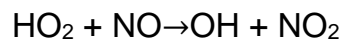
Ozone (O<sub>3</sub>) is the ingredient of photochemical smog and takes large parts of urban oxidant. Because of its extensive health effect, it is concerned as a pollutant and monitored.

### 1.2.1 Ozone formation

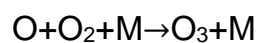
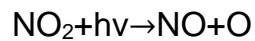
Fig.1.4 show the scheme of tropospheric ozone formation. Firstly, this sequence initiated by the reaction of VOC or CO with hydroxyl radical.



Then followed by conversion of NO to NO<sub>2</sub>



NO<sub>2</sub> is photolyzed to generate atomic oxygen, which combines with O<sub>2</sub> to create O<sub>3</sub>



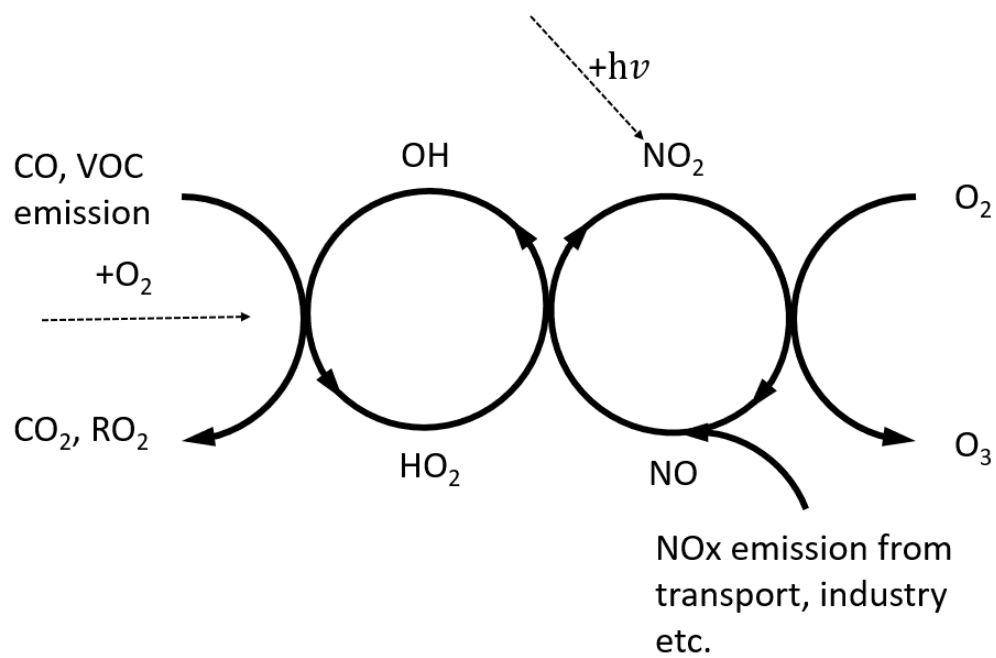


Fig.1.4 Scheme of tropospheric ozone formation

### 1.2.2 VOC-NOx-ozone relationship

Fig.1.5 shows the sensitivity between volatile organic compounds, nitrogen oxides, and ozone formation. From the picture, there are two regimes to be paid attention, VOC limited regime and NOx limited regime.

From Fig.1.4, the formation of tropospheric ozone can be considered by the drive of odd hydrogen radicals. These two regimes represent for two main radical sinks for radicals: nitric acid and peroxides.

Odd hydrogen radicals are composed of OH, HO<sub>2</sub>, and RO<sub>2</sub>. The initial reaction of ozone production depends on the abundance of OH, and OH depends on the source and sink of odd hydrogen radical.

#### 1) VOC limited regime

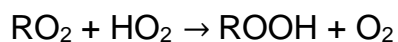
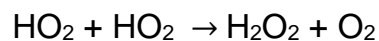
VOC limited regime occurs when the nitric acid presents for the dominant radical sink.



In this case, ambient OH concentration will be determined by the reaction of OH with NO<sub>2</sub>. Because of the rate of nitric formation decrease with the NOx concentration increase, OH concentration will increase. So, the ozone formation increases with the NOx decrease in VOC limited regime.

#### 2) NOx limited regime

NOx limited regime occurs when peroxide is the main dominant radical sink.



In this case, ambient HO<sub>2</sub> and RO<sub>2</sub> concentrations will be determined by the peroxide-forming reactions. The ambient HO<sub>2</sub> and RO<sub>2</sub> concentration vary little because of the rate of peroxide is quadratic in HO<sub>2</sub>. With the abundant RO<sub>2</sub> and HO<sub>2</sub>, the reaction with NO determine the formation of ozone. This

rate increases with the NOx concentration increase. So, the ozone formation decreases with the NOx decrease in NOx limited regime.

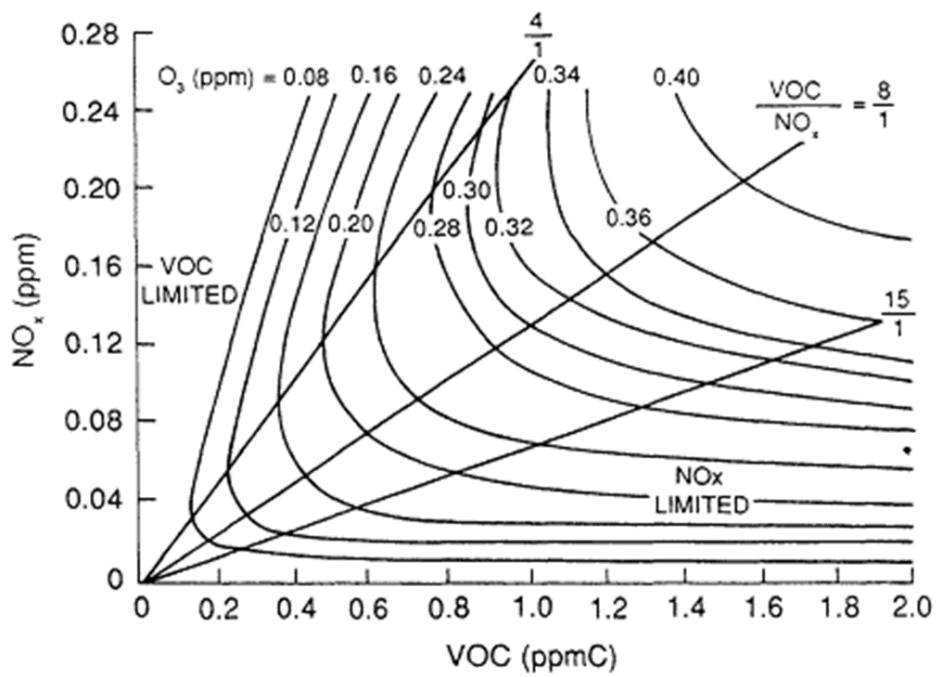


Fig.1.5 The relationship between ozone, VOC, and NOx<sup>[2]</sup>

### 1.2.3 Effect on human health and crops

Many researches have proved that breathing ozone in the air can do harm to human health, especially for people with asthma, elder adults, outdoor workers and children. By constricting the breathing muscles, ozone can cause shortness of breath, coughing, infectious susceptibility and chronic obstructive pulmonary diseases. These symptoms have been found in healthy people, and for sensitive group, such as children and asthma patients, they can be even more serious. <sup>[3][4]</sup>

Many meta-analyses of ozone and mortality has been done by researchers, showing the positive linear relation between ozone concentration and mortality, even at very low pollution level. Robust evidence is found between ozone exposure and mortality when using the background concentration only, typically range from 10 ppb to 25 ppb. Therefore, any anthropogenic contribution to ambient, no matter how slight, will improve the risk for premature mortality risk. <sup>[5][6][7]</sup>

Besides, ground-level ozone also harms plants. In fact, the damage to plants caused by ozone outstand all other air pollutants combined. Ozone enters the leaves by the normal gas exchange. Ozone is such a strong oxidant that cause the chlorosis and necrosis. Apart from the bad looking, it effects the photosynthesis directly, causing the yield loss. Field researches have proved the production loss for economy crops under current seasonal 8-hour ozone concentration, from 40 ppbv to 60 ppbv. <sup>[8]</sup>

### 1.3 Diesel vehicle emission

#### 1.3.1 Emission characteristic

Traditional internal combustion engine used for vehicles can be roughly concluded into two types, the gasoline type and diesel type. Since the different chemical composition of the fuel, petrol engines and diesel engine differ as well. Diesel engines use a cycle reminiscent of a four-stroke cycle, but with compression heating causing ignition, rather than needing a separate ignition system. The advantage of diesel engine is fewer fuel consumption per unit distance, thus generating less carbon dioxide. As a result of directly injected before the power stroke, the fuel can only burn completely when ambient oxygen is sufficient, this leads to the characteristic diesel emission factors.

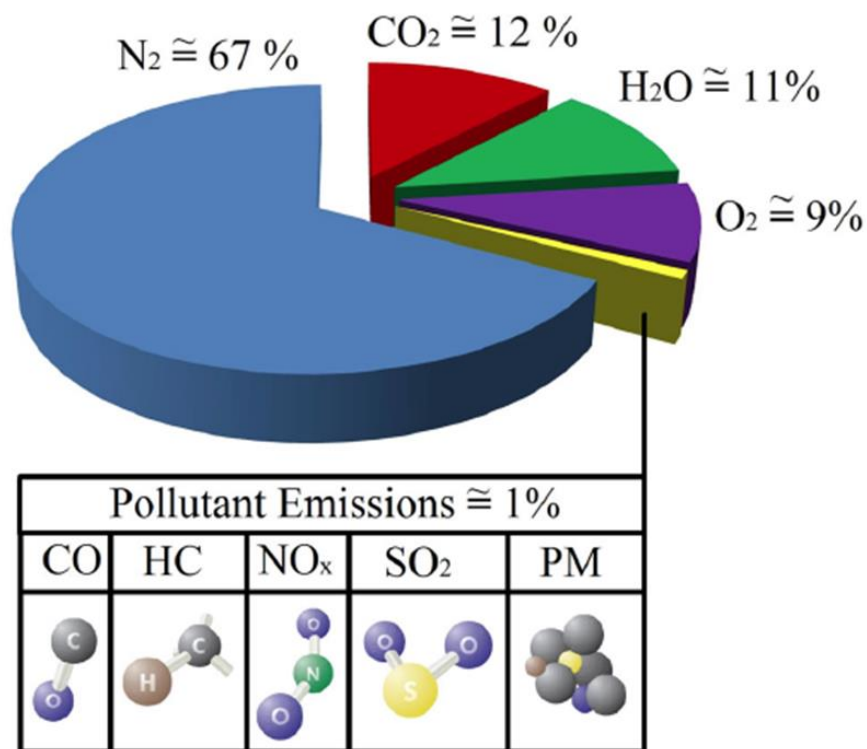


Fig.1.6 Diesel exhaust composition <sup>[9]</sup>

Fig.1.6 shows the approximately composition of diesel exhaust gas. Less than 1 percent of the diesel exhaust gas is pollutant emissions. Since the

diesel engines are lean-combustion designed, the concentration of carbon monoxide and hydrocarbon is minimal. And the amount of sulfur dioxide is mostly depending on the fuel specification and quality. Ultra-low sulfur diesel is provided to prevent harmful effect sulfur dioxide emission. So, the main emission problem comes from the particle matter and NO<sub>x</sub>.

Table 1.2 shows the main pollutant concentration in diesel exhaust. NO<sub>x</sub> and PM emission are far more than the environmental standard.

Table 1.2 Pollutant in diesel exhaust<sup>[9]</sup>

Species	Fraction	Unit
NO <sub>x</sub>	50-1000	ppm
PM	1-30	mg/m <sup>3</sup>
CO	100-500	ppm

Particle matter emission in the exhaust gas are from the incomplete combustion of fuel hydrocarbon. A heavy-duty diesel engine is classified as 41 % carbon, 7 % unburned fuel, 25 % unburned oil, 14 % sulfate and water, 13 % ash and other components. Diesel engines particulate matter emission are considerably higher than that of gasoline engines.<sup>[10][11]</sup>

As mentioned above, highly compressed hot air is used to ignite the fuel. Normally this process generates only water and carbon dioxide. However, the temperature in the cylinders is above 1,600 °C, causing the nitrogen to react with oxygen and generating NO<sub>x</sub> emission. The amount of NO<sub>x</sub> produced is a function of the maximum temperature, residence time and oxygen concentration. Emitted NO<sub>x</sub> is formed in the early process of combustion, for the highest temperature in the cylinder. The relationship between temperature and NO<sub>x</sub> emission has been revealed by , showing that the increase of temperature leads to increase NO<sub>x</sub> emission amount by as much as threefold

for every 100 °C increase. <sup>[12][13]</sup>

Nearly 40-70 percent urban NO<sub>x</sub> is contributed by the road transport. And among multifarious types of emission, diesel vehicles are the most contributors to the emission. Comparing diesel vehicle and gasoline engines, the higher combustion temperature of diesel vehicle make it emit more NO<sub>x</sub> than traditional petrol vehicles. For a single vehicle, the emission is as much as 20 times than a petrol one, and for total amount, diesel vehicle should take responsibility for around 85 percent of all NO<sub>x</sub> emission from mobile source, primarily in NO form. <sup>[14]</sup>

With the development of diesel engine, the efficiency of fuel leads to less incomplete combustion, while the NO<sub>x</sub> emission will increase simultaneously. So, the control of NO<sub>x</sub> emission tends to be a growing problem.

### 1.3.2 Japanese diesel consumption

Table 1.3 shows the 2016 Japanese automobile fuel consumption surveyed by Ministry of Land, Infrastructure and Transport. According to the survey, nearly almost gasoline is consumed by private vehicle. And for diesel, more than 60% are consumed by business vehicle

Table 1.3 Automobile fuel consumption, 2016, Japanese <sup>[15]</sup>

	Business Vehicle	Private Vehicle
Gasoline (10 <sup>6</sup> L)	771	50,438
Diesel (10 <sup>6</sup> L)	16,922	8,536

Table 1.4 shows the consumption for the Kanto area. In the Kanto area, most of diesel is consumed by the business vehicles, which should take responsibility for NOx emission in the Kanto area.

Table 1.4 Automobile fuel consumption, 2016, Kanto <sup>[15]</sup>

	Business Vehicle	Private Vehicle
Gasoline (10 <sup>6</sup> L)	310	13,544
Diesel (10 <sup>6</sup> L)	4,475	2,418

### 1.3.3 Japanese NOx emission

Fig.1.7 shows the proportion of total NOx emission for Japan, 2011. Most NOx emission comes from transport activities. Nearly 20% of total NOx emission is caused by the automobile. Compared to the 35% of 1990, the decrease in NOx emission is quite effective.

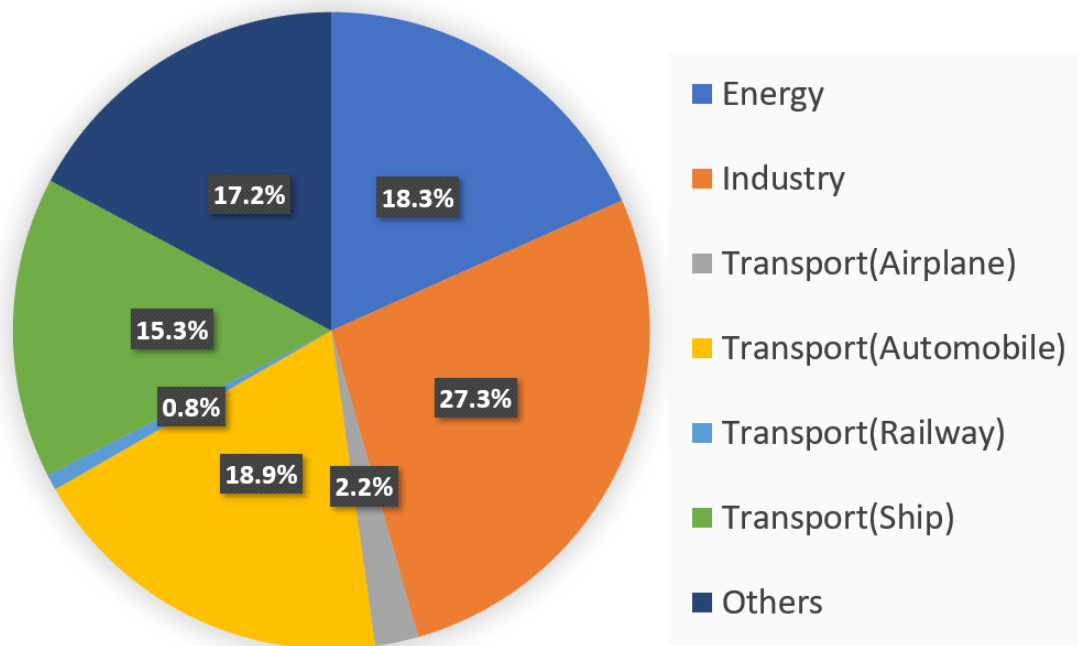


Fig.1.7 Total NOx emission<sup>[16]</sup>

Fig.1.8 shows the automobile NOx emission proportion. Special diesel vehicle means the vehicles used off road, for example, heavy equipment used for constructions like backhoe loader. Although the gasoline emission is nearly twice of it of diesel, the emission of total automobile only takes 13.8%. On the contrary, most of NOx emission comes from diesel vehicles. Normal diesel vehicles take responsibility for 55% of total NOx emission. For further reduction of NOx, unlike currently used urea selective catalytic reduction, a new method of hybrid vehicle can be put into practice.

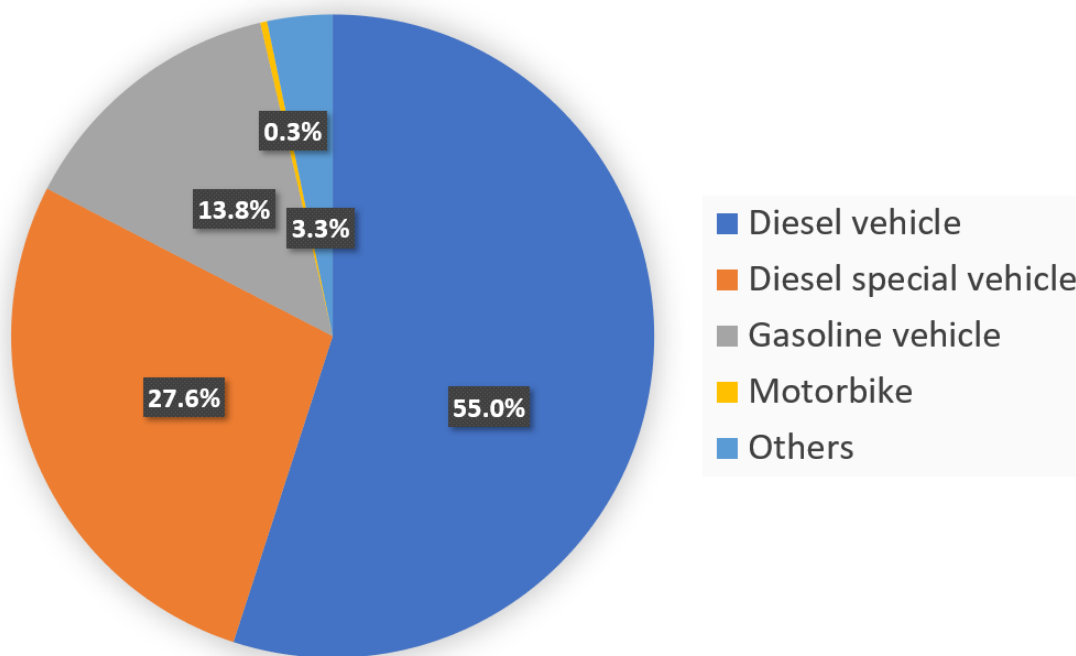


Fig.1.8 Automobile NOx emission<sup>[16]</sup>

## 1.4 Hybrid vehicles

Hybrid vehicles are vehicle powered by two or more type of energy, with more than one actuation system. Generally, the energy comes from fuel, batteries, fuel cells, or suppressed air. And actuation system includes internal combustion engine, electric motor, turbine engine and so on.

The principle of hybrid engine is to take advantage of the best performance of different engines under different speeds. For example, the electric motor can provide better turning power than combustion engines at low speed, and combustion engines are good at maintaining high power at high turning speed. By switching the actuation system in proper time, a better fuel efficiency can be achieved, and fuel consumption can be reduced simultaneously.

For the environmental effects, there are several advantages over traditional vehicle.

1) By using multiple braking system, the energy can be used to charge the batteries, thus reducing the fuel consumption and prolong the life expectancy of vehicles.

2) Taking advantages of different actuation, the fuel efficiency can be improved.

3) Adapting electric motor to assist the internal combustion, the air pollutant can be reduced. Because of the high temperature in the cylinder leads to high pollutant emission, with the assistance of electric motor, time of full power running conditions for internal combustion engines can be reduced, so does the air pollutant emission.

4) Consuming less fuel means the CO<sub>2</sub> emission from fuel combustion will be reduced. Although there are some doubts on the total carbon emission of hybrid vehicle, according to a life cycle assessment report on hybrid vehicle published by the Europe Union, the total carbon emission is less than traditional vehicles under the electricity generation conditions of UK.

## 1.5 Purpose

The hybrid vehicles have the advantages of less fuel consumption, less greenhouse gas emission, and less pollutant emission. But the impacts on the ozone formation are still uncertain due to the fact that sensitivity of VOC-NO<sub>x</sub>-ozone concentration is complicated. This simulation is done to reveal the ground-level ozone concentration change by introducing the hybrid heavy-duty vehicle.

## 2 Calculation methods

In this research, the Weather Research and Forecasting (WRF) Model and the Community Multiscale Air Quality (CMAQ) Modeling System are used for calculating the ground-level ozone concentration. After validating the simulation data and stationary observed data, new emission inventories of hybrid vehicles are adopted for predicting the consequence of introduction of hybrid vehicle to Kanto Area during summer season.

## 2.1 WRF

The Weather Research and Forecasting Model is a next-generation mesoscale numerical weather prediction system designed by the lead of National Center for Atmospheric Research. The WRF is composed of two dynamical cores, a data assimilation system, and a parallel computing program. This model can serve to the meteorological application range from the scale of tens of meters to thousands of kilometers. Simulations can be done from inputting the actual atmospheric conditions from observation and analysis or ideal conditions for prediction.

The WRF is the non-hydrostatic model of complete compression, and the fundamental equations are shown below

Newton's second law

$$\frac{dv}{dt} = -\alpha \nabla p - \nabla \varphi + F - 2\omega \times v$$

where

$\alpha$ : Specific volume,  $1/\rho$

$\varphi$ : Geographic latitude

$F$ : Frictional force

Continuity equation

$$\frac{\partial \rho}{\partial t} = -\nabla \cdot (\rho v)$$

Ideal gas equation

$$p\alpha = RT$$

First law of thermodynamics

$$Q = C_p \frac{dT}{dt} - \alpha \frac{dp}{dt}$$

where

$C_p$ : Coefficient of specific heat at constant pressure

Conservation of water vapor mixing ratio

$$\frac{\partial \rho q}{\partial t} = -\nabla \cdot (\rho v q) + \rho(E - C)$$

where

$q$ : water vapor mixing ratio

$E$ : Represents for evaporation

$C$ : Represents for condensation

Seven equations with seven unknowns, with proper boundary conditions, for example, the surface and top of the atmosphere, it is possible to integrate them, and the weather can be forecasted.

In this study, WRFv3.7.1 was used for meteorological calculation.

## 2.2 CMAQ

The Community Multiscale Air Quality (CMAQ) modeling system is being developed and maintained under the leadership of the EPA National Exposure Research Laboratory.

Air quality models integrate understandings of the complex processes that affect the concentrations of pollutants in the atmosphere. Establishing the relationships among meteorology, chemical transformations, emissions of chemical species, and removal processes in the context of atmospheric pollutants is the fundamental goal of an air quality model (Seinfeld and Pandis, 1998)

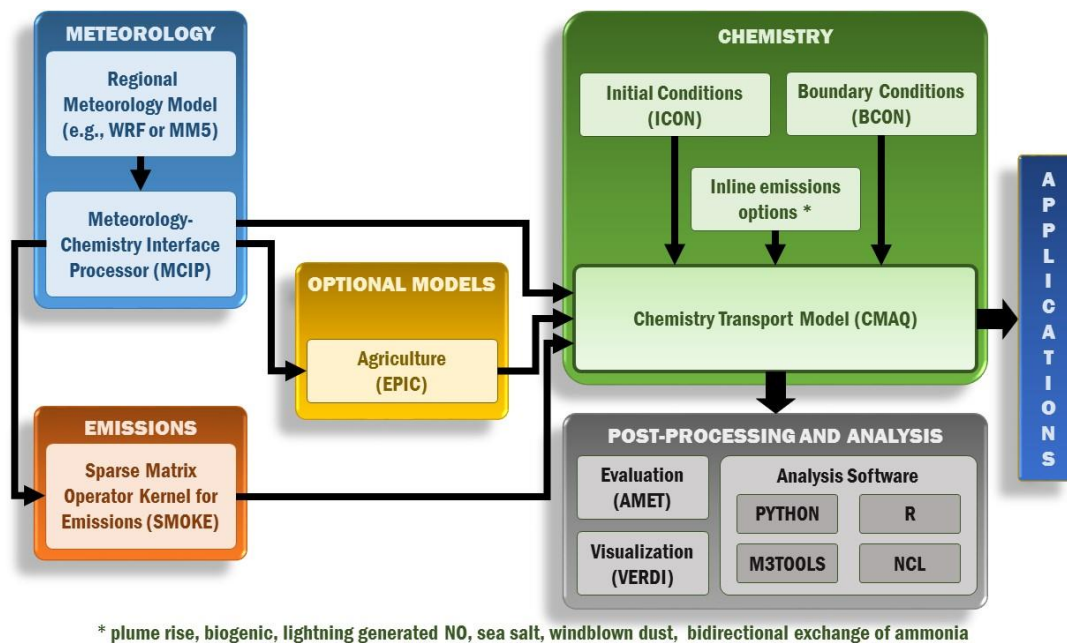


Fig.2.1 CMAQ structure<sup>[17]</sup>

Fig.2.1 shows a simple structure of CMAQ program. We can see three parts of data are necessary for running chemistry transport model.

Meteorology data generated from the WRF determines the physical conditions of chemical reaction, such as solar radiation, humidity, and pressure.

Emission data comes from inventories under different instructions. The more detailed the inventories are, the less errors would have in chemical reaction and transportation. By modifying the emission data, the sensitivity analysis of a certain emission source can be evaluated.

In chemistry part, reaction equations are defined. Aerosol chemistry and gas chemistry are two important parts for atmospheric chemical reactions. Mechanism and kinetics of reactions are defined in the model files. They can be easily modified to the latest research.

Other two important parts are the initial conditions and boundary conditions. Initial conditions show the starting concentration of target species, the beginning of simulation. Boundary conditions are the concentration on the fringe of certain area. Chemical exchange for grid on the boarder of area can be calculated with data. For the largest domain, some global chemical model such as HTAP-2 and MOZART are adapted to get boundary and initial conditions. For the second domain and third domain, these condition can be derived from calculation of parent domains.

The 3-D chemical transport of model of mass concentration can be concluded in to this equation

$$\frac{\partial C_i}{\partial t} + u \frac{\partial C_i}{\partial x} + v \frac{\partial C_i}{\partial y} + w \frac{\partial C_i}{\partial z} = \frac{\partial}{\partial x} \left( k_x \frac{\partial C_i}{\partial x} \right) + \frac{\partial}{\partial y} \left( k_y \frac{\partial C_i}{\partial y} \right) + \frac{\partial}{\partial z} \left( k_z \frac{\partial C_i}{\partial z} \right) + R_i + D_i + S_i$$

where

$R_i$ : Reaction of chemical  $i$

$D_i$ : Deposition of chemical  $i$

$S_i$ : Source emission of chemical  $i$

Paragraphs from left to right represents concentration change, advection, dispersion, diffusion, chemical reaction, deposition and emission sources for

chemical  $i$  respectively. Meteorological prediction for advection, dispersion and diffusion, mechanism for chemical reaction and deposition, detailed inventories for emission sources, the concentration change can be calculated.

The velocity of  $u, v, w$  and the coefficient of dispersion of  $k_x, k_y, k_z$  are derived from the result of WRF meteorological calculation,

In this study, CMAQv5.2.0 was used for chemistry transport calculation.

## 2.3 Calculation Conditions

### 2.3.1 Period

Pollution events with high ozone concentration are highly associated with sunshine and warm temperature. High ozone is very rare when the temperature is under 20°C, quite common with the temperature over 30°C. Besides temperature and sunshine, high ozone concentration conditions appear more easily when relatively wind is light and conditions that vertical mixing in the atmosphere is suppressed because of thermal inversion or subsidence layers.

Concerning these parameters, the simulation is conducted for two weeks, from 2013-7-21 to 2013-8-3, as shown in Table 2.1.

Table 2.1 Meteorological data from 2013/7/21 to 2013/8/3<sup>[18]</sup>

Date	Air pressure/kPa	Rainfall/mm	Temperature/°C			Humidity/%		Wind velocity/m/s		Sunshine duration/h
			Average	Highest	Lowest	Average	Lowest	Average	Lowest	
7/21	1007.6	--	24.8	29	21	62	51	2.5	5.6	8.7
7/22	1005.2	0	26.5	30.4	23.5	77	64	2.8	6.5	6.1
7/23	1002.3	24.5	28	35.2	25.2	76	44	2.2	7.5	5.9
7/24	1001.4	1.5	25.4	27.1	24.3	85	78	2.6	4.8	0
7/25	1000.3	0	26.7	29.3	24.1	80	68	1.5	3	0
7/26	1000.2	--	28.4	32.3	25.5	76	61	2.7	5.3	5.1
7/27	1000.2	19.5	27.6	33.1	22.3	77	59	3	7.8	5.2
7/28	1002.2	0.5	27.3	31.8	22.9	71	54	2	4.3	8.1
7/29	999.4	7	26.3	27.3	24.9	83	73	2.1	4.6	0
7/30	996.8	0	27.8	31.2	25	78	63	2.5	5.6	2.3
7/31	999.6	0	27.4	30.7	25.2	77	65	2.7	5.6	0.8
8/1	1000.1	0.5	27.5	32.8	24.2	80	59	2.4	5.7	3.2
8/2	1004.7	0	25.6	29.1	23	73	61	2.6	5.3	4
8/3	1005.2	--	26.7	30.8	23.5	68	53	2.5	5	6.6

From Table 2.1 we can see the meteorological data of Tokyo for the simulation periods. During these period, most of the highest temperature are above 30°C, which are quite ideal for the ozone formation. Wind are not so strong that ozone can accumulate easily.

### 2.3.2 Domain

Before simulation, it is necessary to define the calculation area. For both quickness and preciseness requirement of calculation, generally from the largest to the target region, three domains are defined.

Fig.2.2 shows the nesting of calculation area.

Domain 1 is the whole east Asia, and its grid size is 45 km × 45 km. This domain is calculated because the advection of pollutant from continent has affected the air quality significantly. Besides, warm and humidity wind from Indian Ocean and Pacific Ocean in summer are highly associated with rainfall and cloud formation for Japan. Calculated conditions can be used as the initial and boundary condition for next simulation.

Domain 2 is the whole Japan, with a grid size of 15 km × 15 km. With a smaller grid size, pollutants transported from continent are calculated by a more precise form.

Domain 3 is the target area, Kanto area. Grid size is 5 km × 5 km.

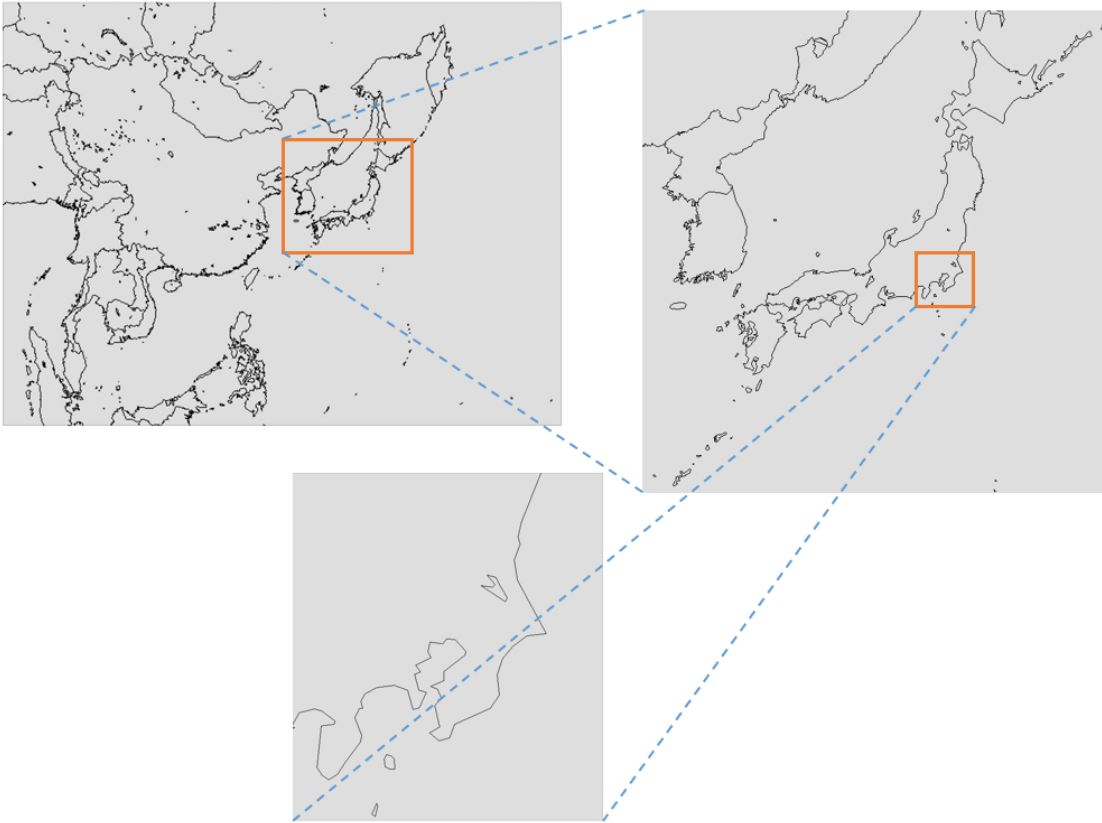


Fig.2.2 Domain nesting of simulation area

### 2.3.3 Emission inventory

The inventory of vehicle emission is made under the instruction of JEI-DB (Japan Auto-Oil Program Emission Inventory Data Base). Except for automobile emission, stationary sources, biogenic volatile organic emission, and volcano is also included. For the necessary requirement of atmosphere simulation, this inventory is not just the total amount of emission, but the monthly, hourly changing pollution data of the 1-kilometer grid.

Inventories for biogenic volatile organic compounds are derived from Model of Emissions of Gases and Aerosols from Nature (MEGAN) version 2.1.

Inventories for volcano are derived from Japan Meteorological Agency, mainly for Mt. Asama, Miyakejima, and Mt. Aso.

#### 2.3.4 Scenario

Three scenarios are adopted for the calculation. One scenario is the base scenario, for validating the simulated data and stationary observed data. Other two scenarios are the introduction of diesel hybrid vehicles (hybrid scenario 1) and diesel hybrid vehicles with gasoline hybrid emission factors (hybrid scenario 2).

According to the JEI-DB (Japan Emission Inventory-Data Base), the vehicle emission consists of six parts: diurnal breathing loss, hot soak loss, running emission, running loss, start emission, and the particulate matter from friction.

Diurnal breathing loss is the permeation of long-time parking and hot soak loss is the permeation that evaporates after daily use, until the temperature of tanks and pipes go down to the ambient temperature. Running loss emissions are evaporated gasoline emissions occurring while a vehicle is driven due to the heating of the fuel and fuel lines. These three types of emission can be derived to the tank design, pipe material, and canister capacity.

Running emission is the exhaust of engine strokes. Start emission is the exhaust when the engine starts to work, depending on the initial conditions of the engine.

Friction is due to the friction between tire and ground, tire and brake block. Particulate matters, usually PM10 is generated during this process.

Since this research is focus on the exhaust change by introducing hybrid power engine, the change of evaporation of fuel and friction particles are ignored, only focusing on the emission of running and start.

Tables 2.3 and 2.4 show the emission factors from chassis dynamometer experiment conducted in Tokyo Metropolitan Research Institute for Environmental Protection. Emission factors mean the emission of pollutant on the assumption that the original emission is 1. Emission factors of diesel hybrid vehicles and gasoline hybrid for NOx and non-methane hydrocarbon are listed.

Table 2.3 Diesel hybrid emission factors

	NOx	NMHC
Cold start emission	0.918	0.050
Run emission	0.992	0.126

Table 2.4 Gasoline hybrid emission factors

	NOx	NMHC
Cold start emission	0.140	0.256
Run emission	0.339	0.467

From the table, we can see the NOx reduction rate of diesel-hybrid vehicle is much less than that of gasoline-hybrid vehicle, as a result, the final simulation of diesel hybrid introduction scenario is not so straight. So, the gasoline emission factor is also adapted, assuming that with the technology improvement the effectiveness of diesel-hybrid vehicle can reach current gasoline-hybrid level.

## 3 Result and discussion

### 3.1 Model Validation

Validation is done for the capital cities of seven prefectures of the Kanto Area, Tokyo, Kanagawa, Chiba, Saitama, Tochigi, Gunma and Ibaraki. The validation of this simulation is concluded in two parts, the correlation validation and preciseness validation.

#### 3.1.1 Correlation

Correlation validation is to compare the changing trend of base observed data and calculation data for base scenario, to verify the calculation data can reflect the fluctuation of pollutants.

Figs.3.1 to 3.7 show the tendency validation for 7 prefectures capital cities. Figs.3.1 to 3.4 exhibit the hourly ozone concentration comparison of simulation data and observe data of southern part of the Kanto area. The correlation coefficients of four cities range from 0.610 to 0.726, quite high for the field of simulation. For the first several hours, the model needs a small period of warming up, thus causing some errors for Tokyo and Kanagawa. And from July 28th to July 31st, the sun duration time is relatively short compared with other days. But the solar radiation for these days is overestimated, and because the solar radiation is quite an important factor for oxidant formation, the simulation data is much more than observed data. And for these four cities in the southern part of Kanto area, the concentration transitions are like observed data.

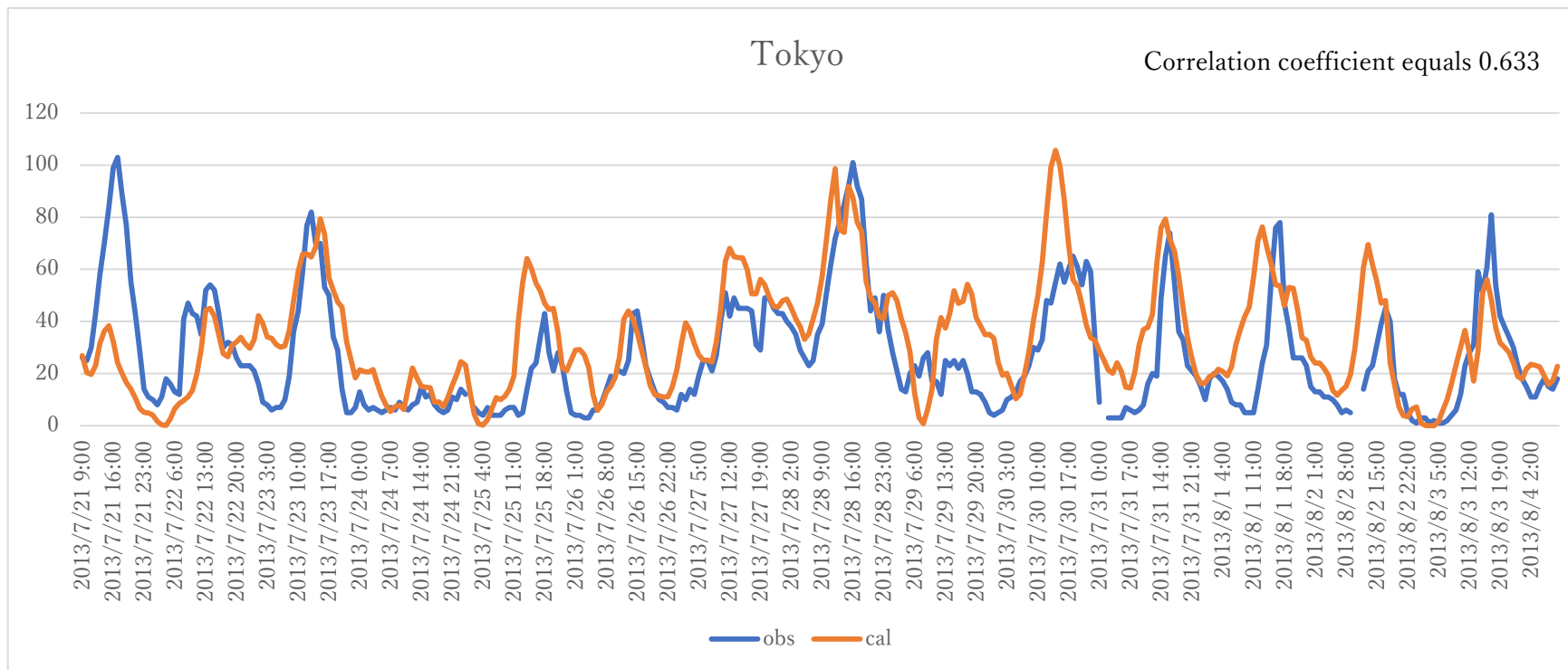


Fig.3.1 Comparison of hourly ozone concentration for Tokyo

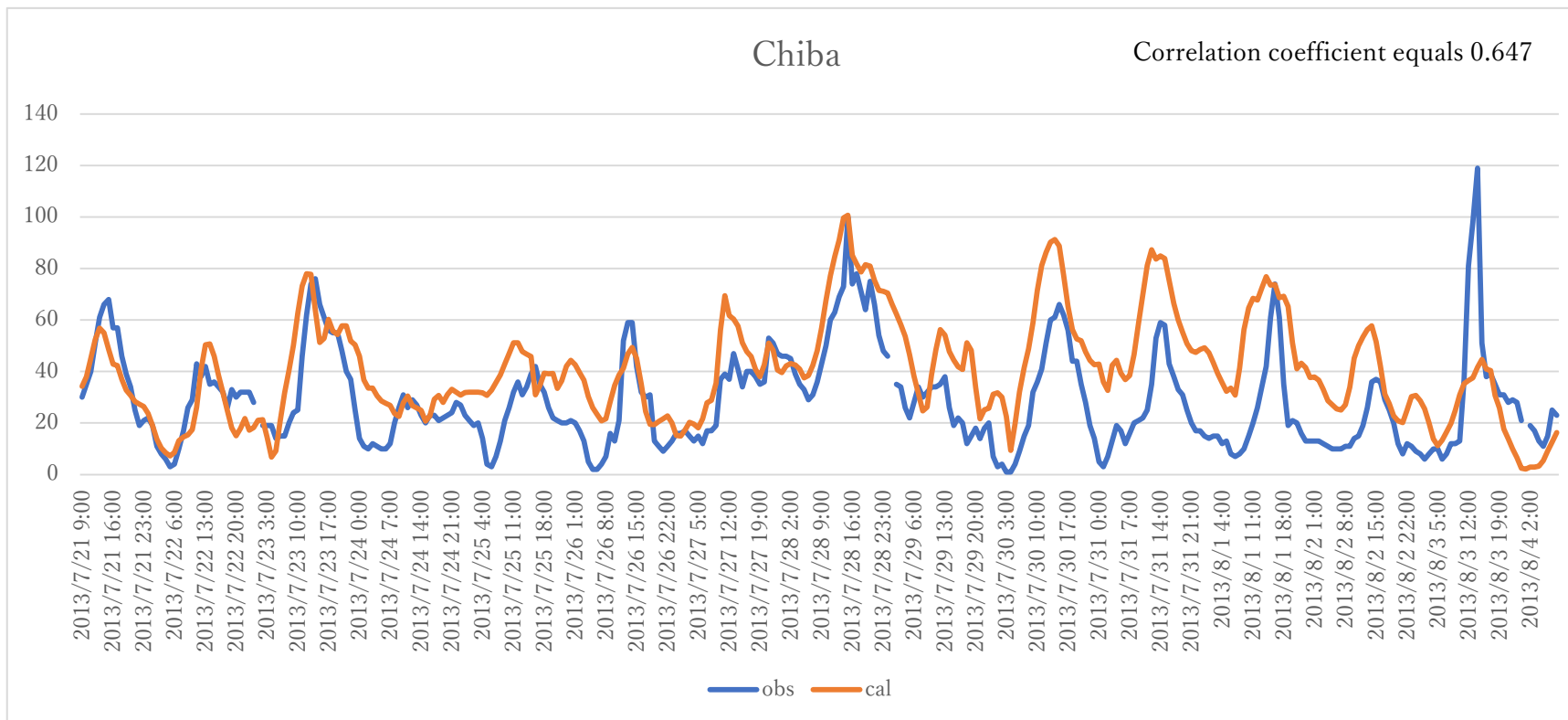


Fig.3.2 Comparison of hourly ozone concentration for Chiba

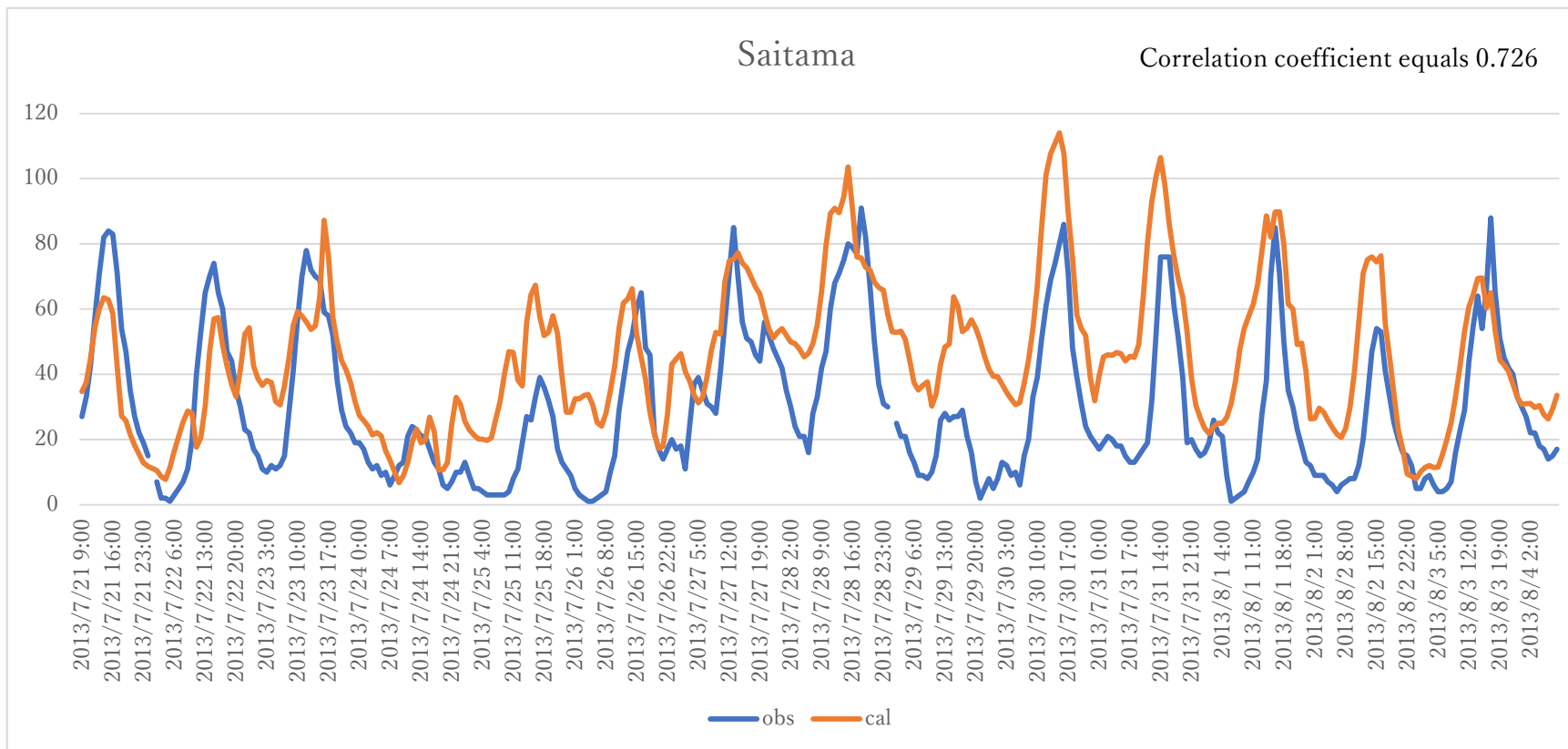


Fig.3.3 Comparison of hourly ozone concentration for Saitama

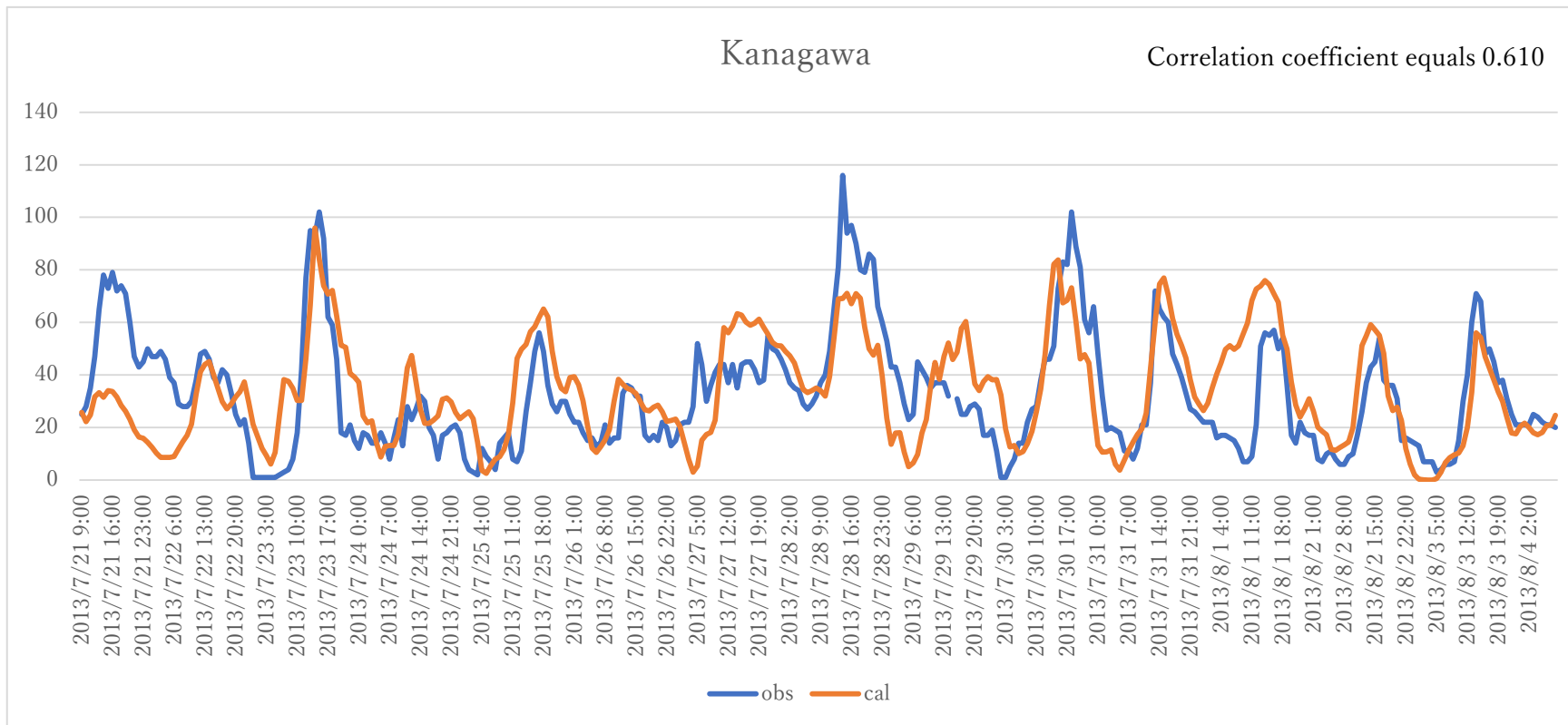


Fig.3.4 Comparison of hourly ozone concentration for Kanagawa

Figs.3.5 to 3.7 show the hourly ozone concentration comparison of simulation data and observe data of northern part of the Kanto area. The differences between the simulation data and observed data are obviously, most of simulation data are overestimated. The correlation coefficient ranges from 0.484 to 0.626.

For the northern cities, because of the rather high pressure of summer sea surface, the sea breeze effect is strong, transporting the urban originated air mass to northern part. The oxidant of downwind area is supposed to be higher than urban area, in the simulation this phenomenon is reflected. And the overestimation of oxidant may be caused by the poor reproducibility of problems on ozone formation during the dispersion and transportation of air mass. Same phenomenon was reported by other researchers' model performance evaluation for the Kanto area<sup>[19][20]</sup>. Besides, the ozone concentration for nighttime is also estimated. This tendency is reported by the research for American urban area and rural area, possible reason is the problem on nighttime NO<sub>x</sub> reproducibility.

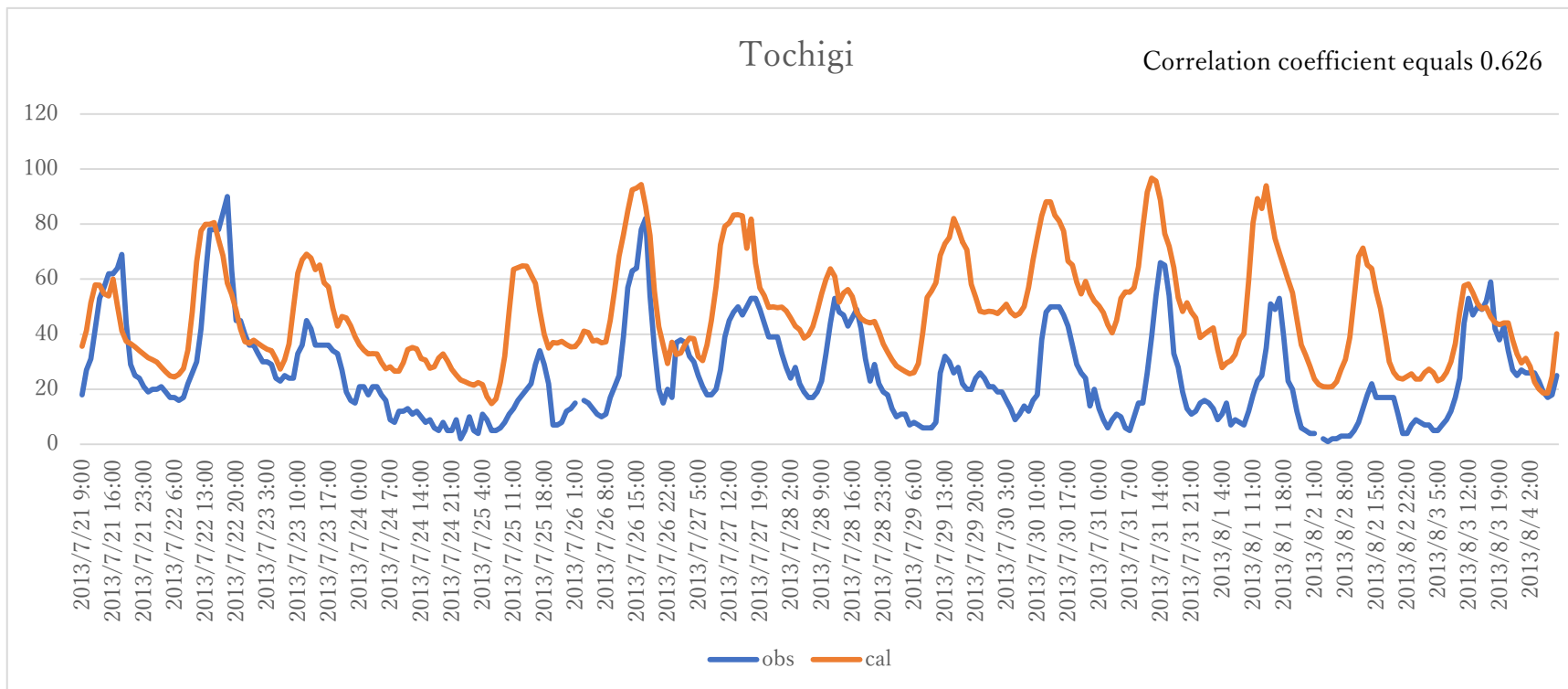


Fig.3.5 Comparison of hourly ozone concentration for Tochigi

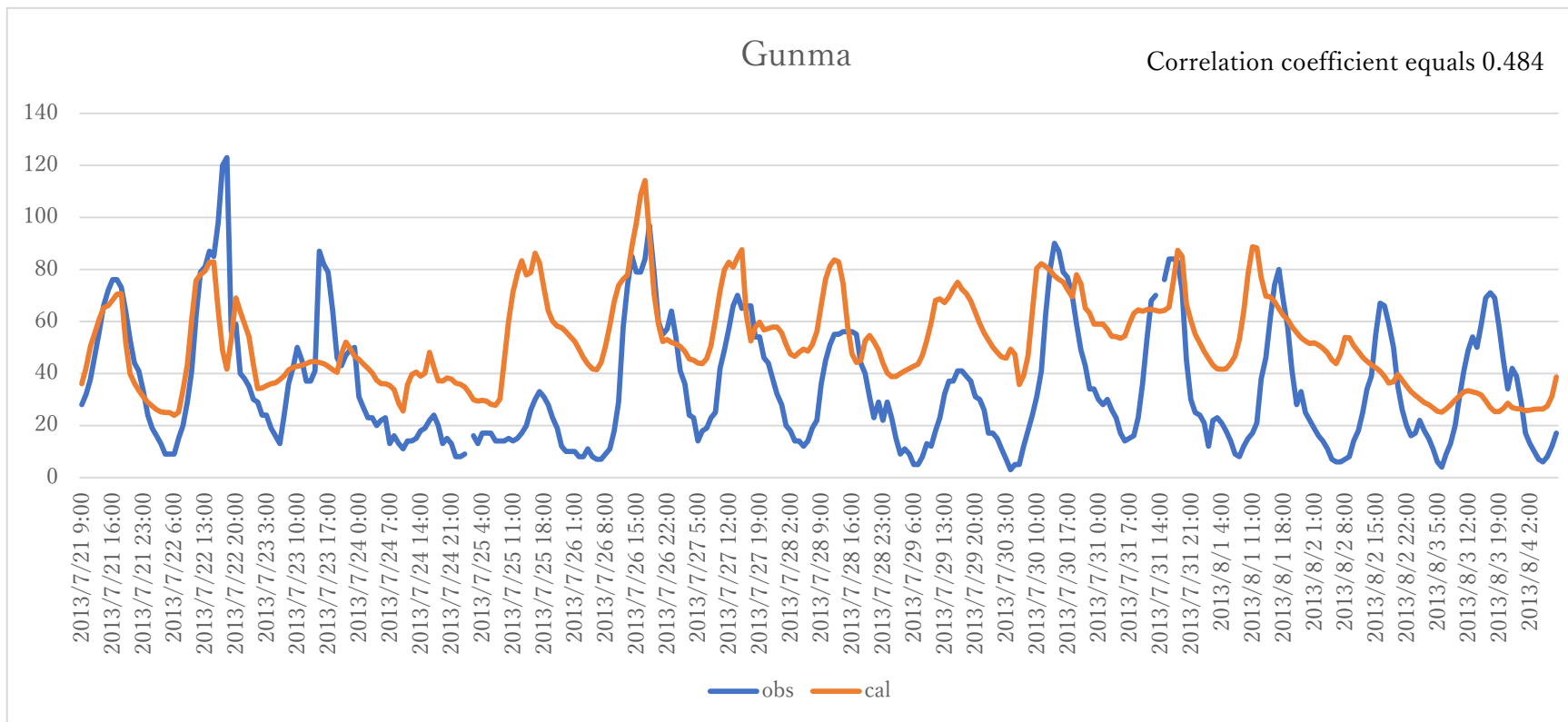


Fig.3.6 Comparison of hourly ozone concentration for Gunma

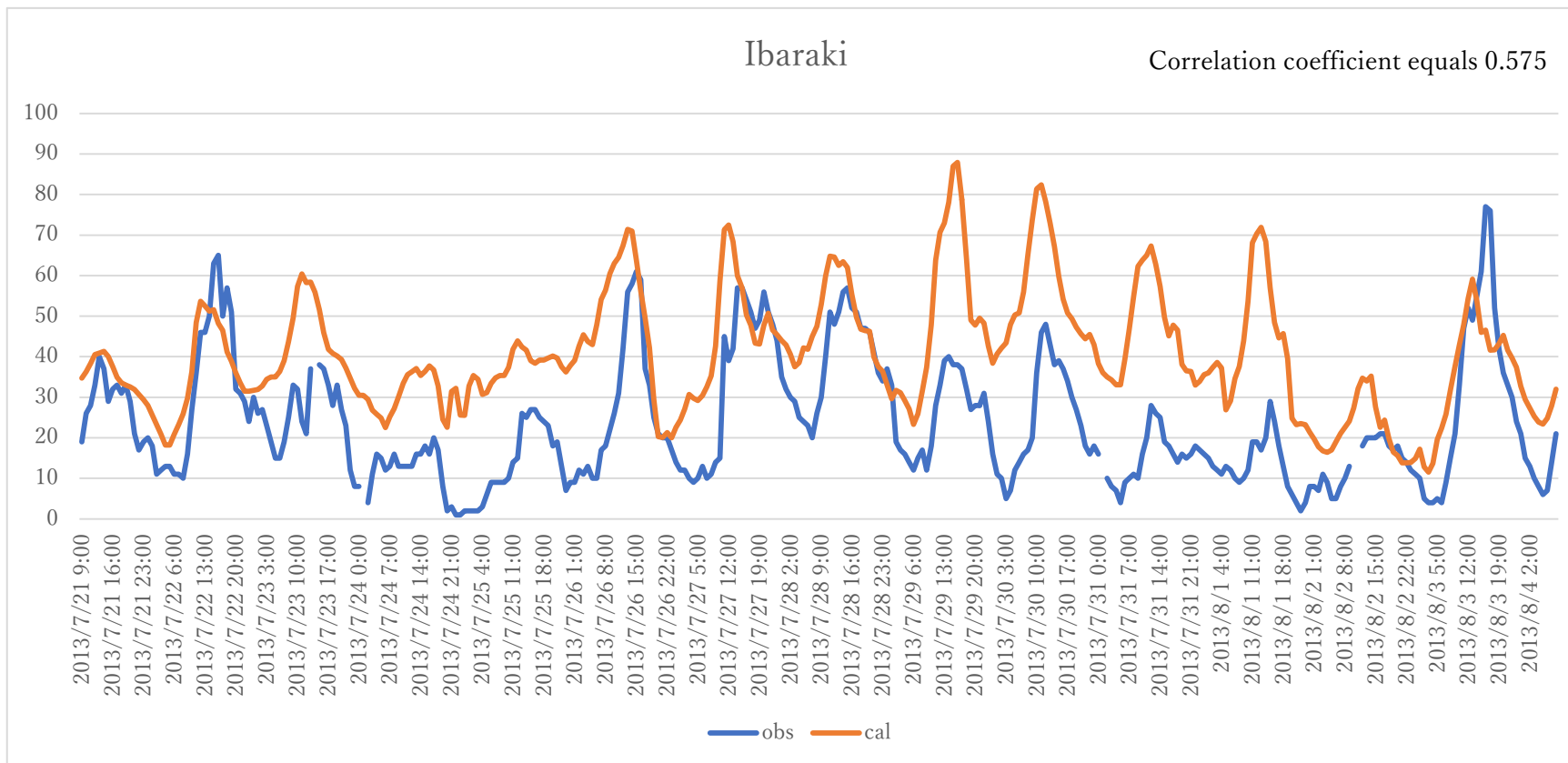


Fig.3.7 Comparison of hourly ozone concentration for Ibaraki

### 3.1.2 Preciseness

Preciseness validation is to compare the observed data and simulated data. The comparison is shown in the scatter plot with three base lines: 1:1, 1:2 and 2:1. X axis means the observed data, Y axis means the calculation data. The more near the plot is to the 1:1 line, the more precise is the simulation. And if the plot is located between the two lines of 1:2 and 2:1, it shows this data is meaningful for the simulation.

Figs.3.8 to 3.14 show the preciseness validation for 7 prefectures capital cities.

The preciseness evaluation can be also concluded southern urban area and northern rural area.

For the urban area, plots are located on the both sides of 1:1 line, evenly and randomly. And most plots are between the two dash lines, meaning acceptable for simulation.

For the rural area, the plots are not evenly. Almost all ozone concentration simulation of Tochigi and Gunma are more than 20 ppbv, 10 ppbv of Ibaraki, while low ozone concentrations are observed in the area above. Besides, most of plots are in the upper part of graph, meaning that the simulation concentration is higher than observed concentration nearly all the time. There are several possible reasons for this phenomenon. One reason, as mentioned above, the overestimation of ozone formation during the progress of dispersion transportation. Other one reason is the effect of NO<sub>x</sub> titration ( $\text{NO} + \text{O}_3 = \text{O}_2 + \text{NO}_2$ ) for rural area is underestimated, which is crucial in the reduction of ozone. Besides, the transportation model for mountain area and the change of biogenic volatile organic compounds caused by climate change should also be considered.

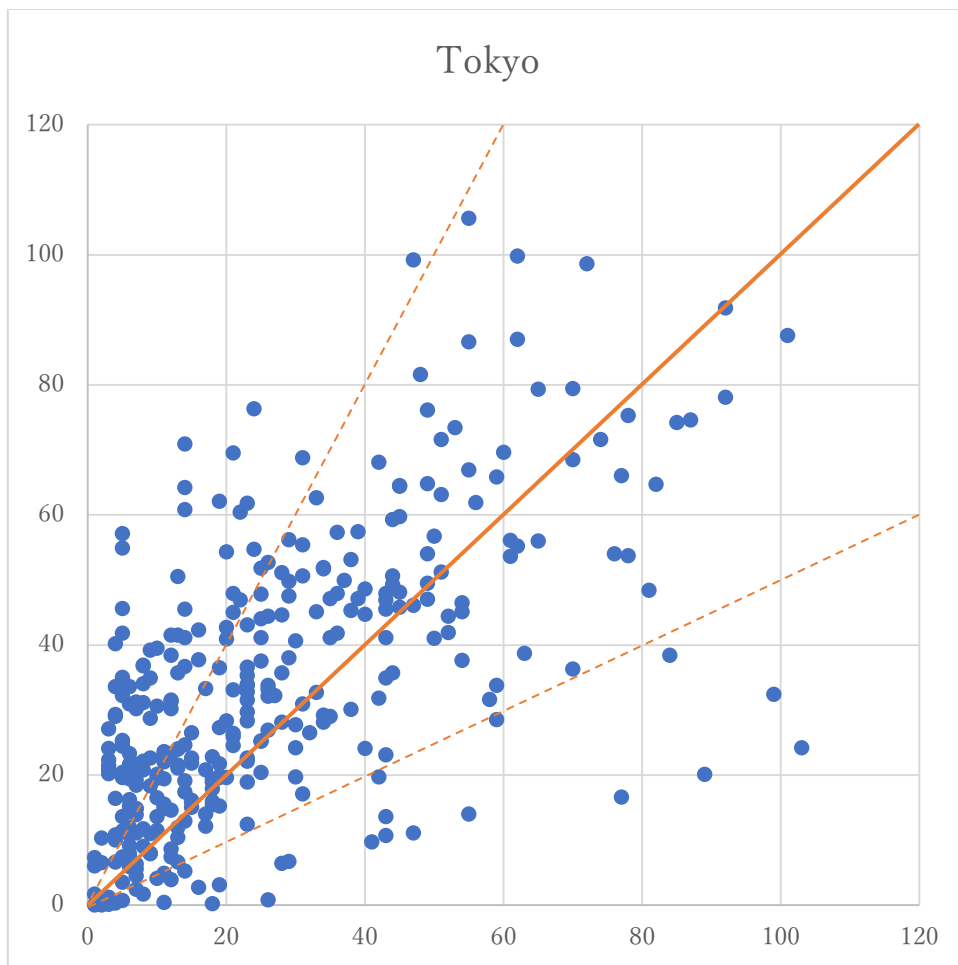


Fig.3.8 Scatter plot of ozone concentration for Tokyo

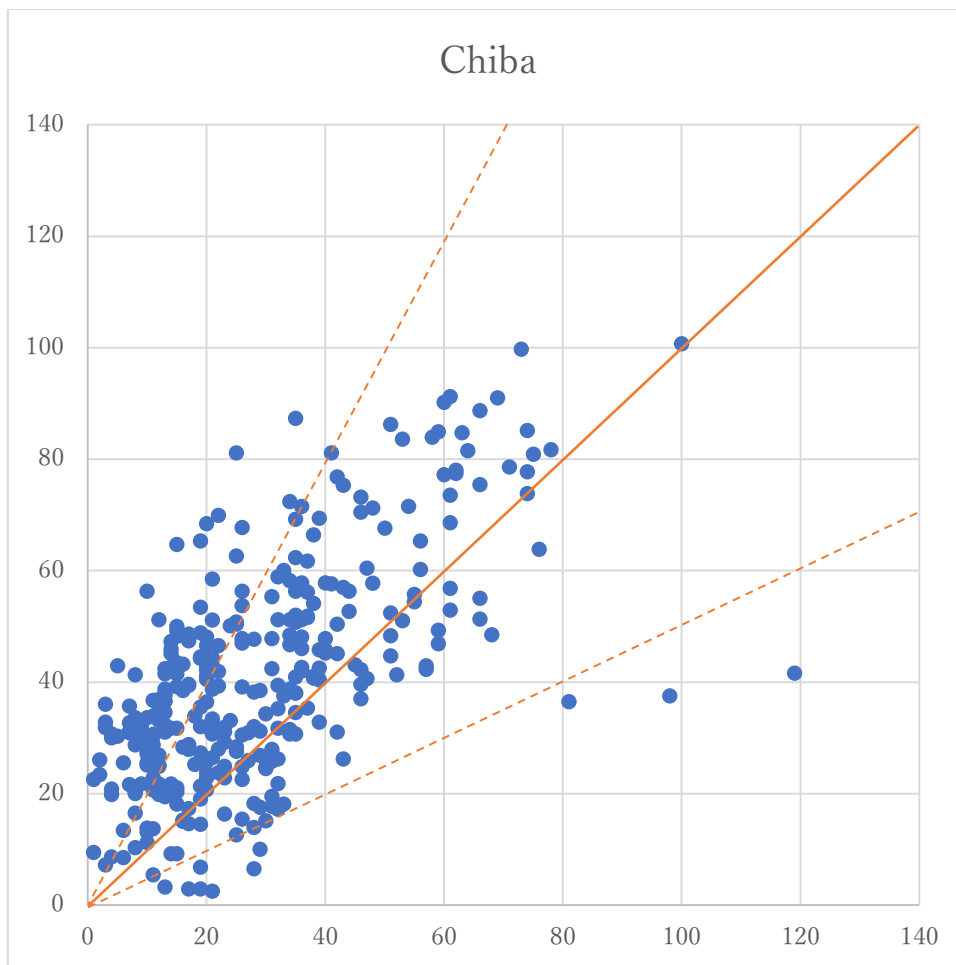


Fig.3.9 Scatter plot of ozone concentration for Chiba

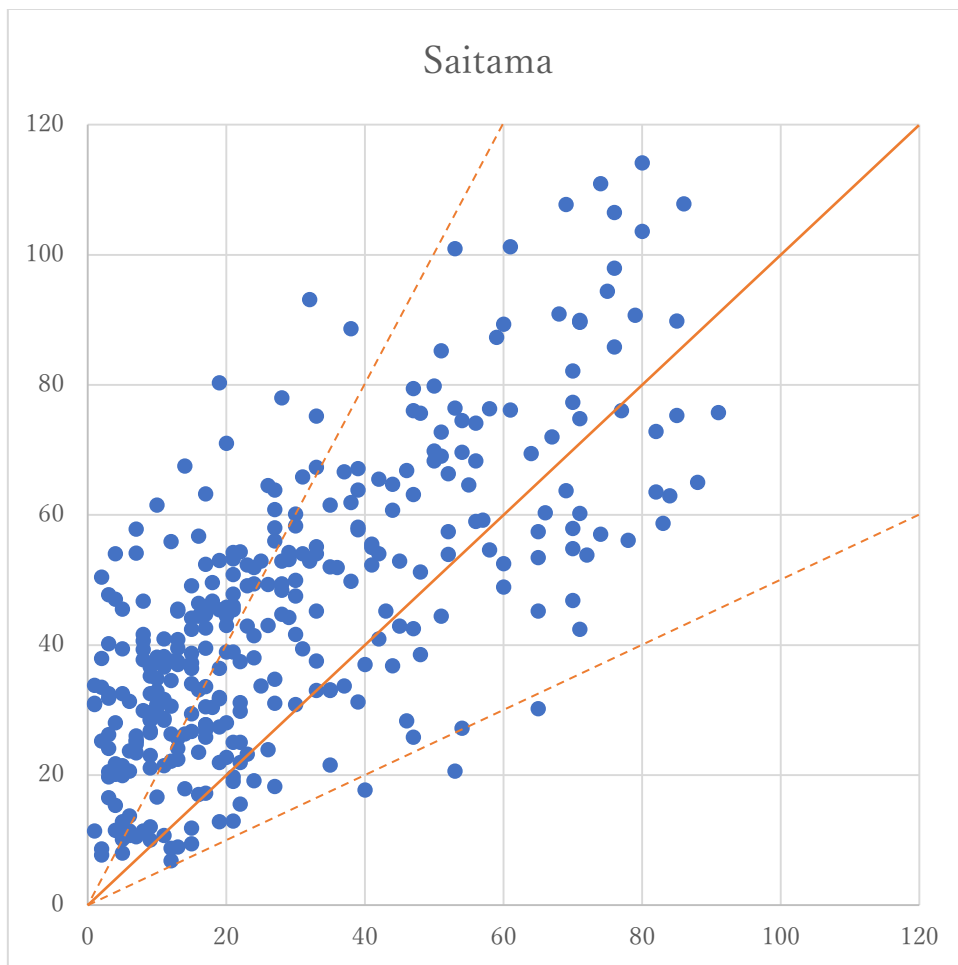


Fig.3.10 Scatter plot of ozone concentration for Saitama

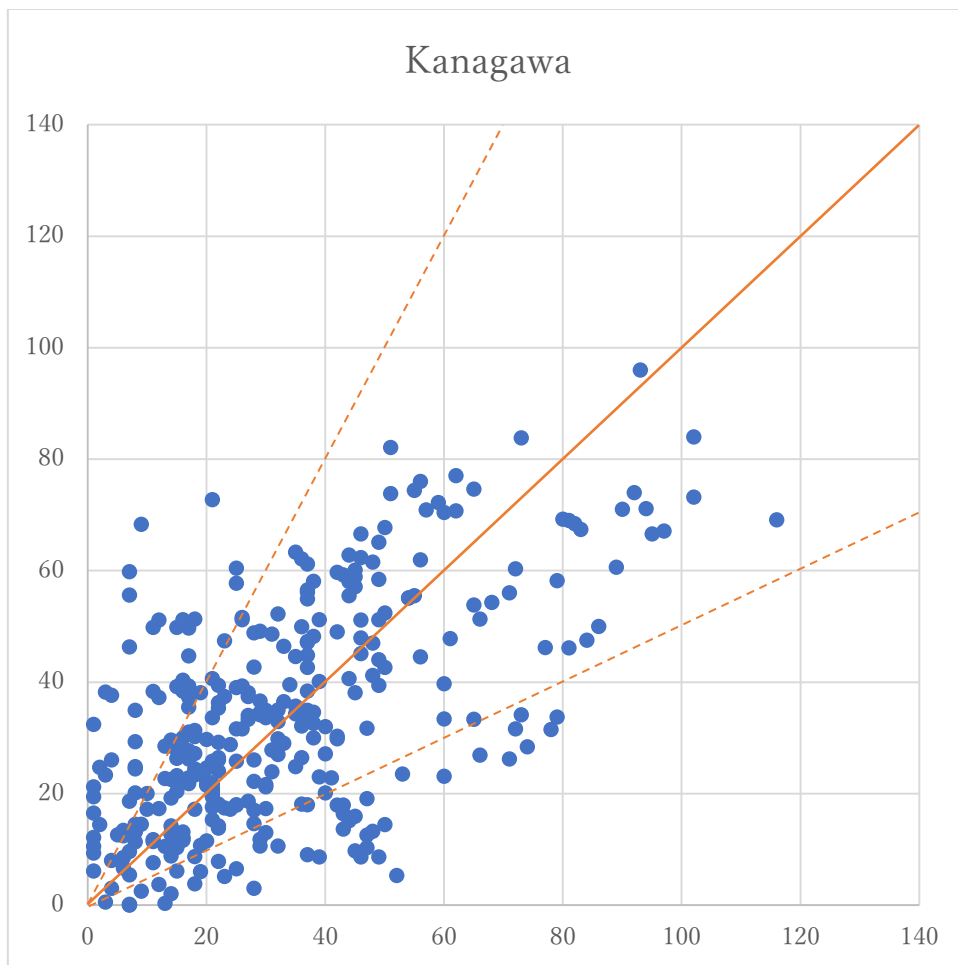


Fig.3.11 Scatter plot of ozone concentration for Kanagawa

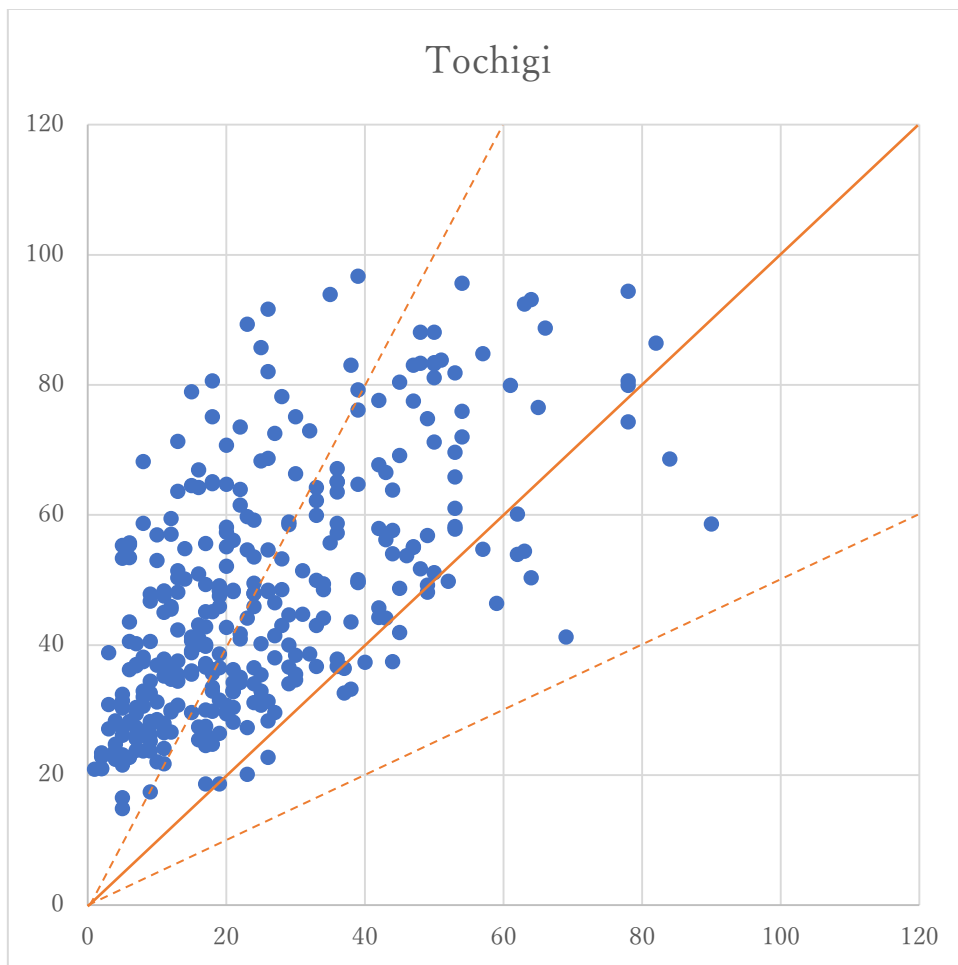


Fig.3.12 Scatter plot of ozone concentration for Tochigi

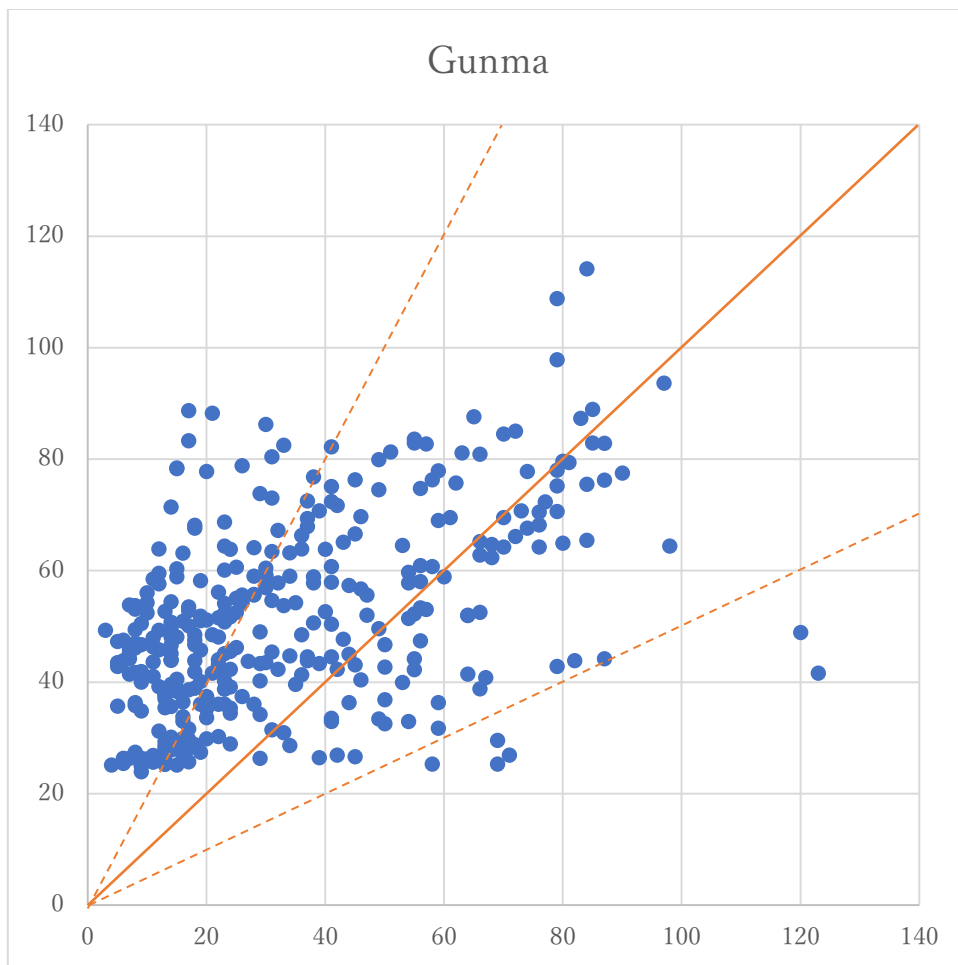


Fig.3.13 Scatter plot of ozone concentration for Gunma

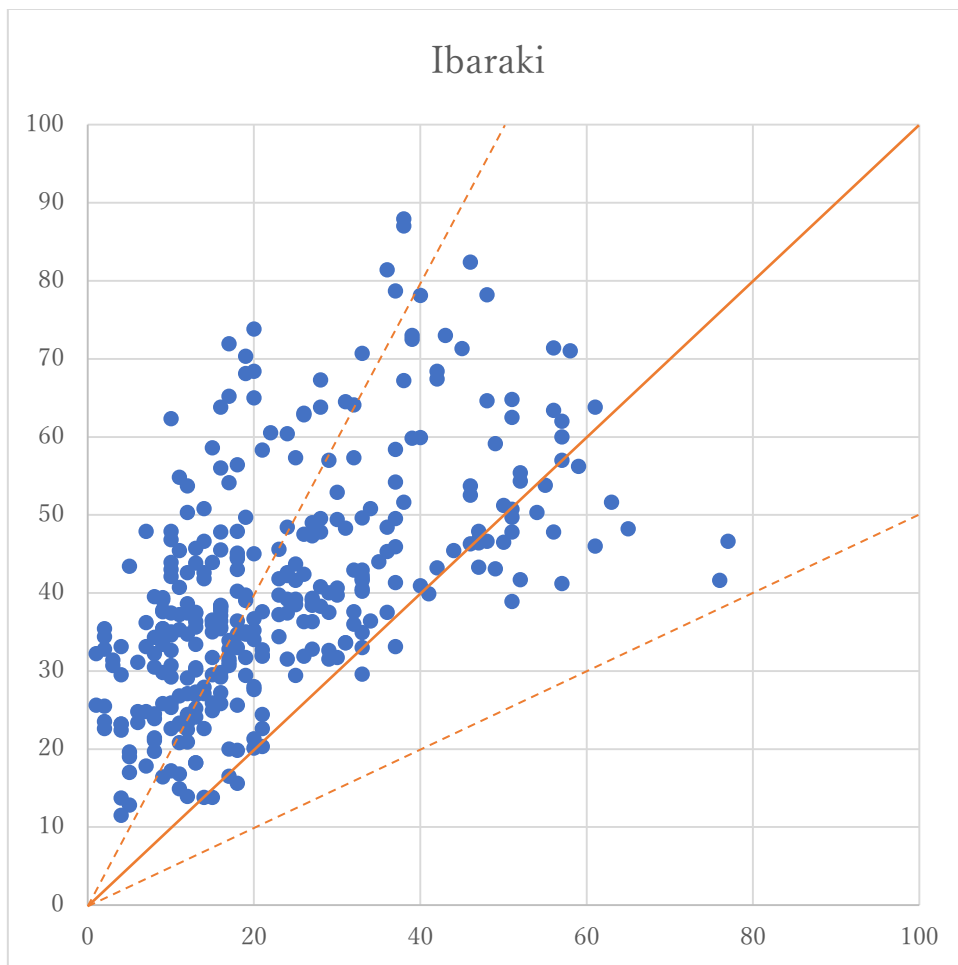


Fig.3.14 Scatter plot of ozone concentration for Ibaraki

### 3.2 Ozone concentration change

By using the CMAQ model, pollutants concentrations for every grid and every hour is calculated. By comparing the concentration calculated by base scenario and hybrid scenarios, the effects on replacing traditional diesel high duty vehicle would be shown directly. The ozone concentration change between scenarios is analyzed for the case of space and time.

### 3.2.1 Spatial distribution

Fig.3.15 shows the ozone concentration change of spatial distribution, hybrid scenario 1. The color series show concentration change after the scenario calculated. In the central part of Kanto area which is typical city terrain, the ozone increased. And the northwest and west part of Kanto area, covered by forest and affected by the sea-land breeze pollution transportation from urban area, the ozone concentration slightly decreased. Ozone changing pattern is in contrast of urban area and suburban area, however, the absolute value of ozone change is relatively small compared with background ozone level. The largest ozone concentration increase is 0.057ppbv, simulated near the Yokosuka city, meanwhile 2013 average annual ozone concentration is 47ppbv. So, under current diesel hybrid emission factors, the ozone concentration changes are meaningful in the aspect of mathematic, the effect on the environment and human beings can be ignored.

Fig.3.16 shows the ozone concentration change of spatial distribution, hybrid scenario 2. In this case, with a higher NO<sub>x</sub> reduction ratio, the pollutant emission and oxidant concentration vary significantly. Referring to the satellite map, it is very straight that for the land covered by vegetations, average ozone concentration decreases, and for the concrete urban terrain, the concentration increases. And specially, the ozone concentration has a strange increase in Tokyo bay, further discussion will be done in chapter 3.2.3.

From Fig.3.17, in the northwest direction of Tokyo, the ozone concentration is higher. As mentioned above, because of the pollutant transportation by the sea-land breeze, ozone concentration is higher in the downwind direction. With the reduction of NO<sub>x</sub> emission, environmental issues for those area are mitigated. Urban area has a better atmospheric quality than downwind area, however, the reduction of NO<sub>x</sub> would aggravate its environmental issues.

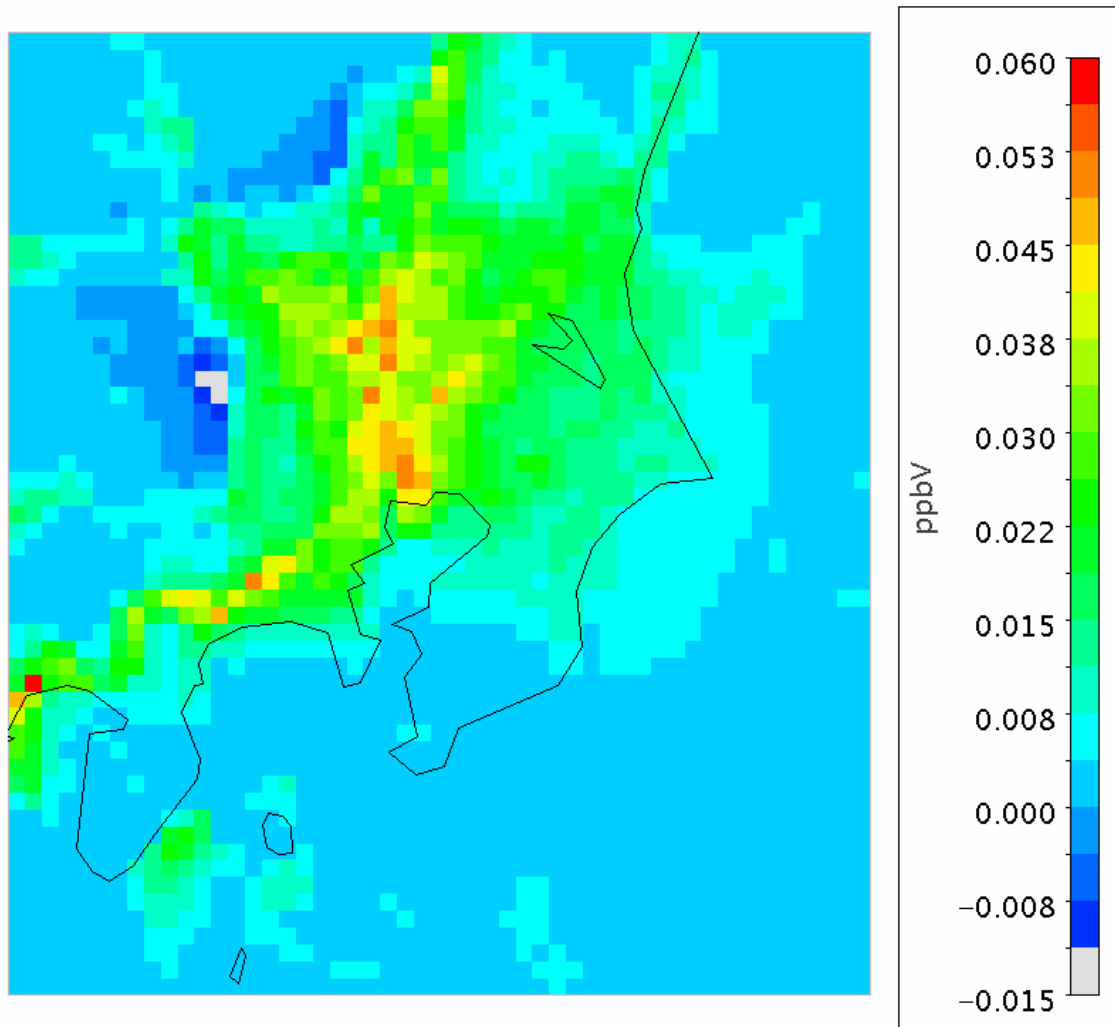


Fig.3.15 Ozone concentration change for Scenario 1

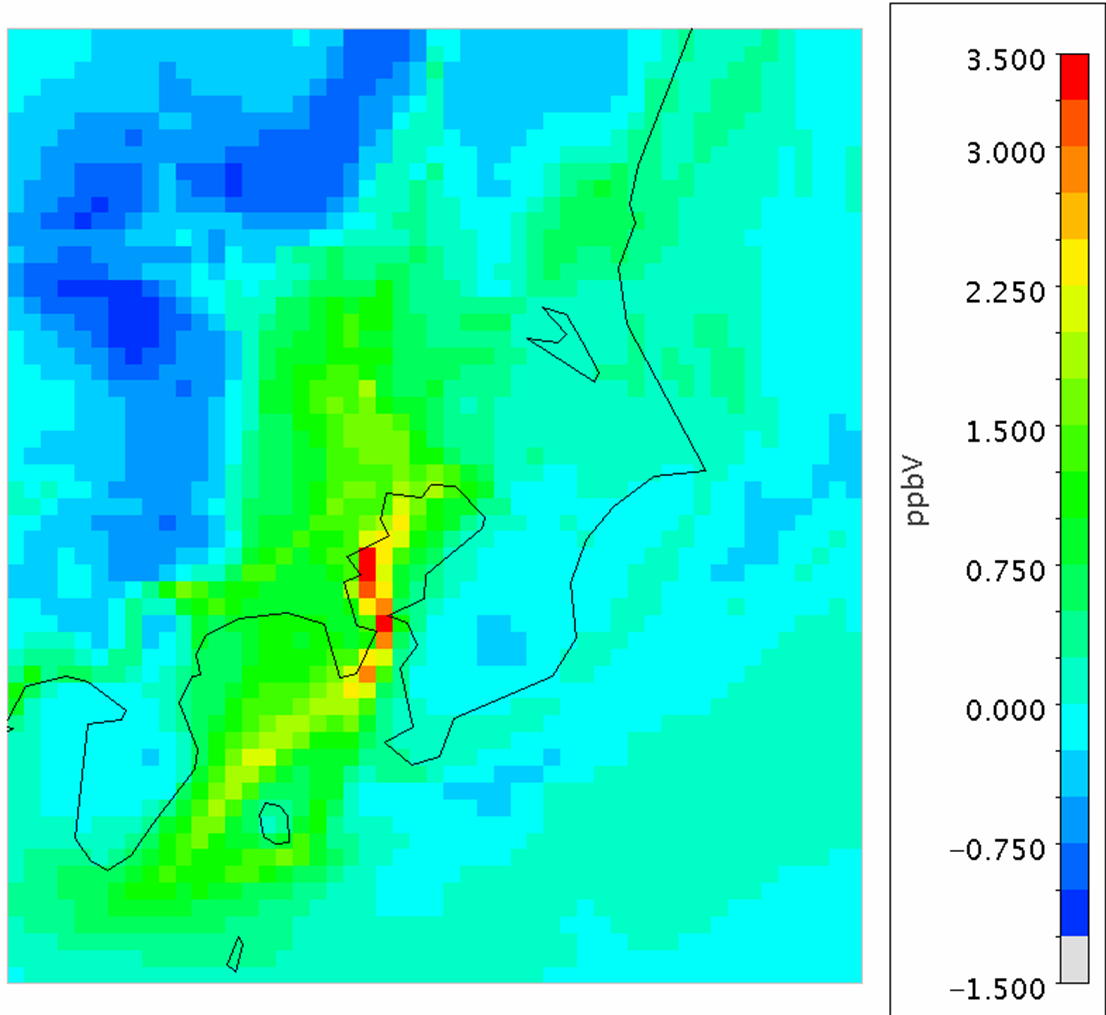


Fig.3.16 Ozone concentration change for Scenario 2

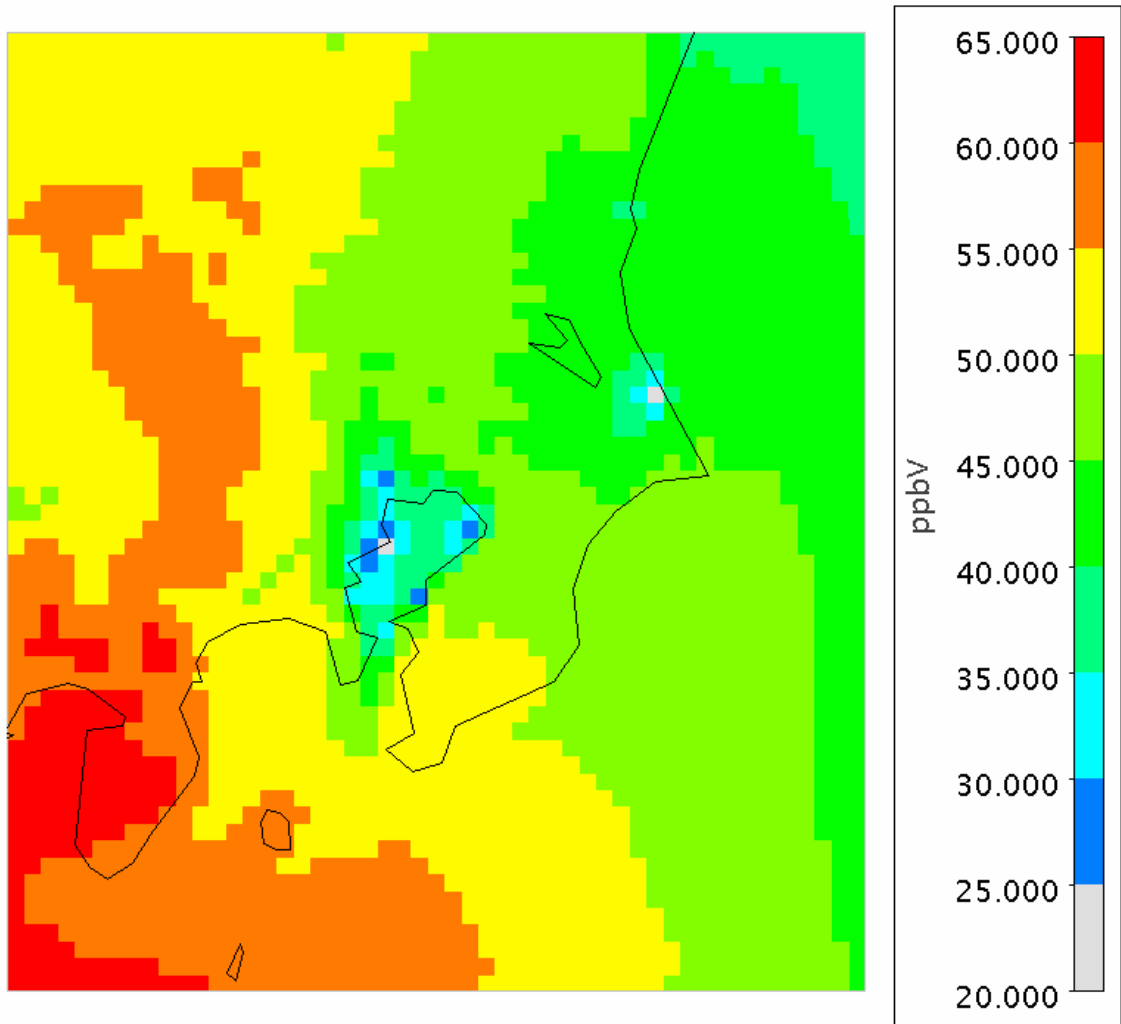


Fig.3.17 Base scenario ozone average concentration

### 3.2.2 Time series

The graphs of time series aim to show the hourly change of ozone concentration for a certain area. Unlike the spatial distribution, the time series graph focuses more on the ozone change for day time and night time, looking forward to explaining the reason for ozone concentration change for a certain area.

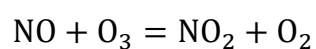
Three cities are selected for time series analysis: Tokyo, Maebashi, and Tateyama.

Tokyo represents for typical urban area.

Maebashi represents for the rural area with the downwind sea-land breeze effect.

Tateyama represents for rural area without pollutant transporting event.

Figs.3.18 to 3.20 show the hourly ozone concentration change. Fig.3.18 is hourly ozone concentration change of Tokyo, the average concentration increased. This can be also shown in its time series graph. In fact, the hourly change of Tokyo fluctuates a lot. For the day time, it is hard to draw conclusion because of the complicated conditions for urban area pollutant formation. There is concentration increase peak from July 28<sup>th</sup> to July 31<sup>st</sup>, the simulation data for these days are not in good correlation with observed data, however. The most possible reason is the meteorological simulation for this period is not so perfect, thus affecting the photochemical reaction. Besides, Tokyo area locates in the area of VOC limited regime, the reduction of NO<sub>x</sub> is less effective on mitigating ozone formation. Hourly change for night time is more regular. From 0 a.m. to 6 a.m., photochemical reaction is restrained for the lack of solar radiation, so the change of ozone concentration is because of the NO<sub>x</sub> titration.



Most of NO<sub>x</sub> are in the form of NO, with the reduction of total NO<sub>x</sub>, the

formula above moves left, leading to the increase of night ozone concentration.

Fig.3.19 is hourly ozone concentration change of Maebashi, the average ozone concentration decreased. Affected by the downwind transporting pollutant, the changes of hourly concentration are more regular and significant. Night time ozone concentration increases because of the same season of NO<sub>x</sub> titration balance move. Daytime ozone concentration decrease in Maebashi is very significant, because Maebashi is in the NO<sub>x</sub> limited area. Most of its NO<sub>x</sub> pollutant are not emitted locally, transported from upwind area instead. The decrease of NO<sub>x</sub> is rather effective on ozone burden. It also shows that the pollutant transportation of urban contributes a lot to rural air quality deterioration. Combining the slight increase of nighttime and great decrease of daytime, the average ozone of Maebashi has an obvious decrease. Although average ozone decreased, the absolute ozone concentration of Maebashi is still higher than that of Tokyo. The introduction of hybrid vehicle mitigates the environmental issues for downwind rural areas, with the cost of making urban air issues severe

Fig.3.20 is hourly ozone concentration change of Tateyama, the average ozone concentration decreases slightly. Different from Maebashi, Tateyama locates in the southeast part of Tokyo gulf, the pollutant from Tokyo is hard to be transported to this area, so the ozone concentration change for this area is more ideal without the advection disturbance. With low NO<sub>x</sub> concentration, the effect of NO<sub>x</sub> titration is rather small, night time concentration keeps stable. And for day time photochemical reaction, referring to the NO<sub>x</sub>-VOC-ozone sensitivity, under low NO<sub>x</sub> concentration and abundant biogenic volatile organic compounds, the decrease of NO<sub>x</sub> is effective for ozone reduction. In conclusion, the introduction for hybrid vehicle improve air quality in term of ozone for isolated rural area.

$\Delta O_3$ /ppbv

Tokyo

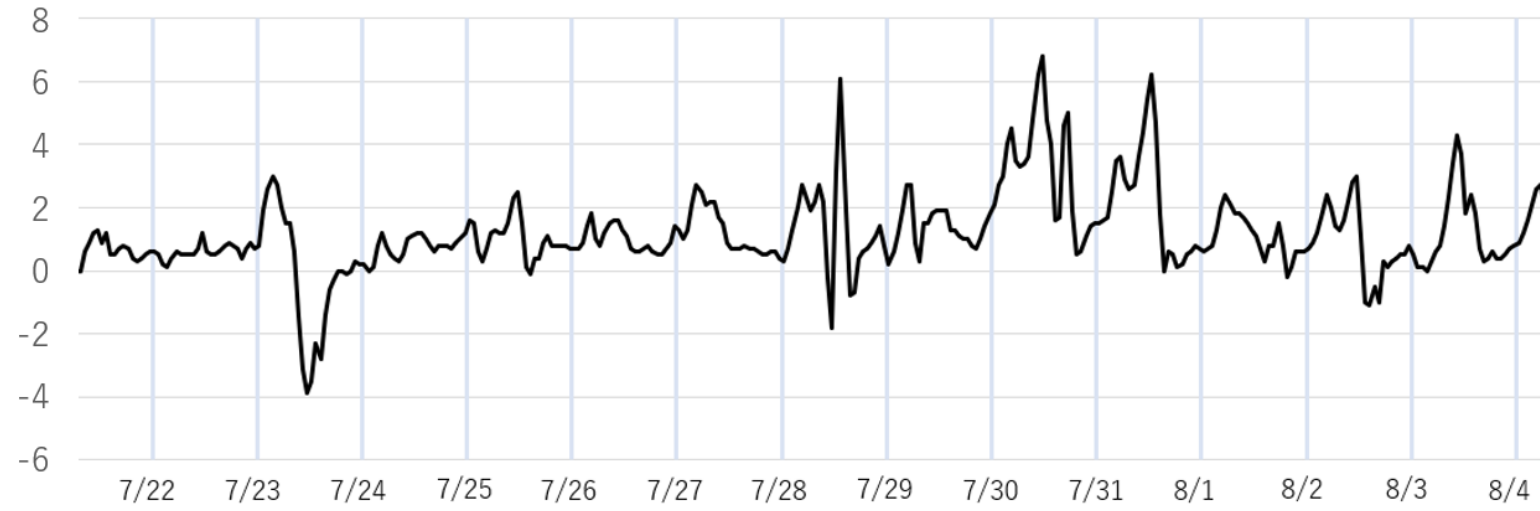


Fig.3.18 Hourly ozone concentration change for Tokyo

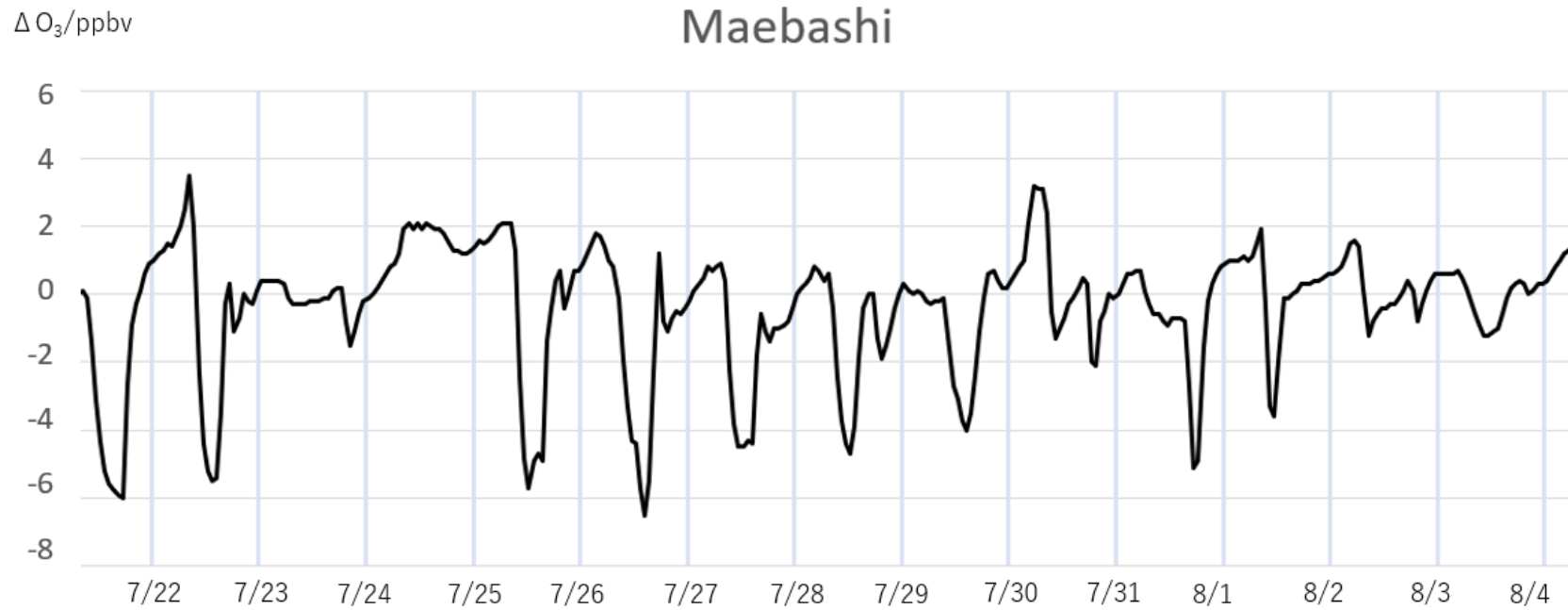


Fig.3.19 Hourly ozone concentration change for Maebashi

$\Delta O_3/\text{ppbv}$

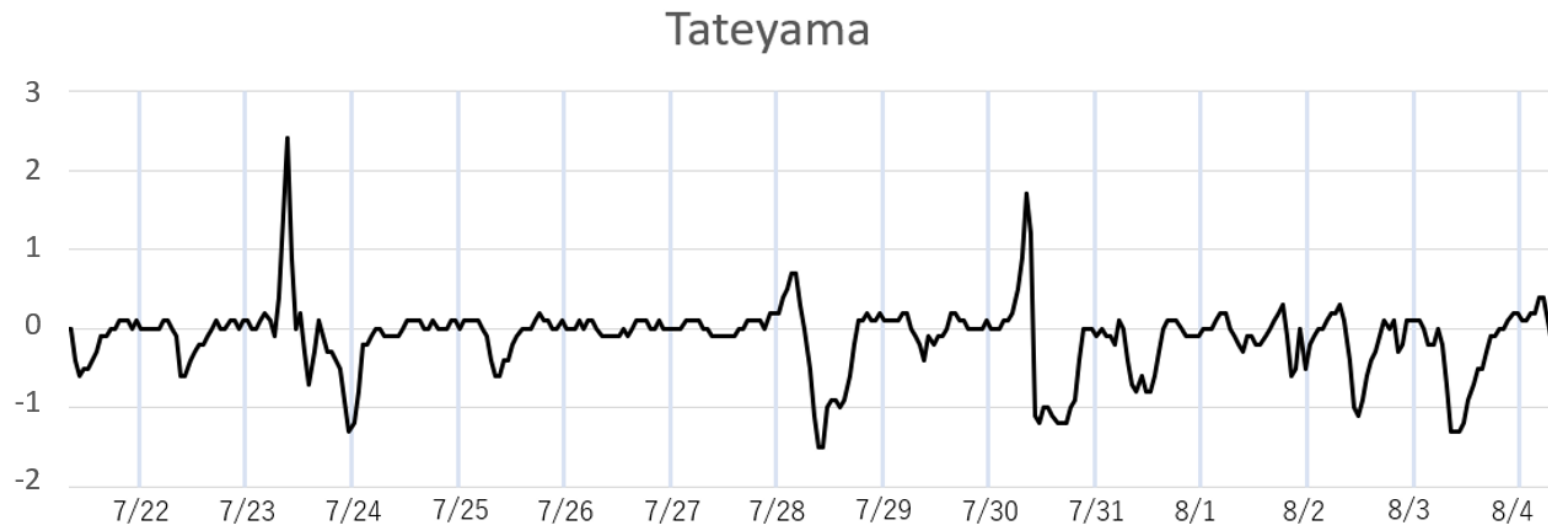


Fig.3.20 Hourly ozone concentration change for Tateyama

### 3.2.3 Ozone increase in Tokyo Bay

From Fig.3.16, the ozone concentration increases strangely from the central Tokyo Bay to the southwest direction. For in this calculation, only emission from heavy-duty vehicles are modified, there must be some reasons for the ozone increase of sea surface.

Figs.3.21 and 3.22 show the hourly ozone concentration change of the highest two mesh on the sea surface.

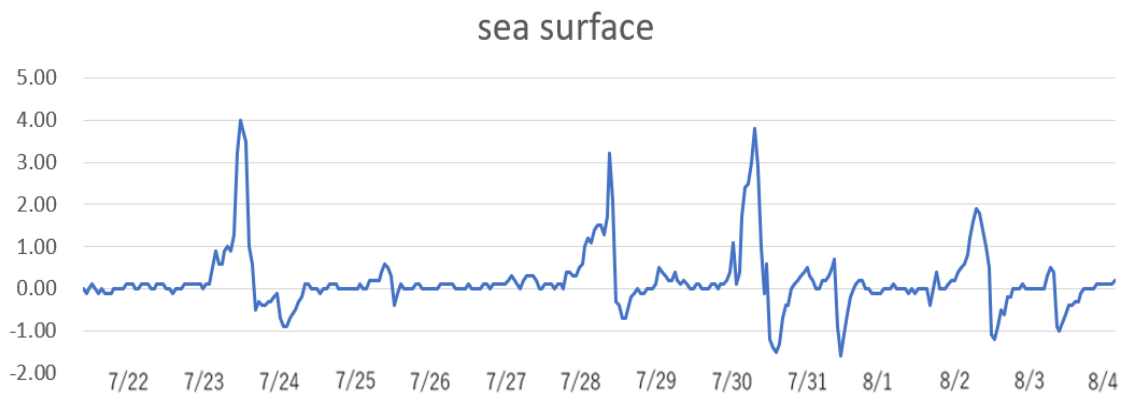


Fig.3.21 Hourly ozone concentration change for highest mesh



Fig.3.22 Hourly ozone concentration change for second highest mesh

The concentration change trend for those two meshes are very similar, there are four main ozone concentration increase on July 23<sup>rd</sup>, 28<sup>th</sup>, 30<sup>th</sup>, and August 2<sup>nd</sup>, from midnight to the noon. Comparing with Fig.3.20, the ozone concentration increase periods are very similar. It means that for the area where NO<sub>x</sub> emission from heavy-duty vehicles are not so high, the ozone concentration changes with the same pattern. And for the sea surface, the main NO<sub>x</sub> emission comes from ship transport, and for Tateyama, main emission from heavy-duty is not so significant as well. This similarity in NO<sub>x</sub> emission leads to the similar changing pattern.

There are four similar peaks on ozone concentration, by checking the calculation data, the reason for the increase are similar, so here just discuss the increase on July 30<sup>th</sup>. From Figs.3.21 and 3.22, the ozone concentration change starts to increase from 0 a.m., reach the peak at noon and fall. This is the typical changing trend of NO<sub>x</sub> titration.

Figs.3.23 and 3.24 show the NO<sub>x</sub> concentration for both base scenario and hybrid 2 scenario, 8 a.m. in the morning. NO<sub>x</sub> concentration spatial distributions are similar, and for hybrid 2 scenario, the NO<sub>x</sub> concentration is less than that of base scenario. And by checking the wind trend of that day, the wind blew to the southwest direction, transporting the high NO<sub>x</sub> emission air parcel from Tokyo Metropolitan area to the sea surface.

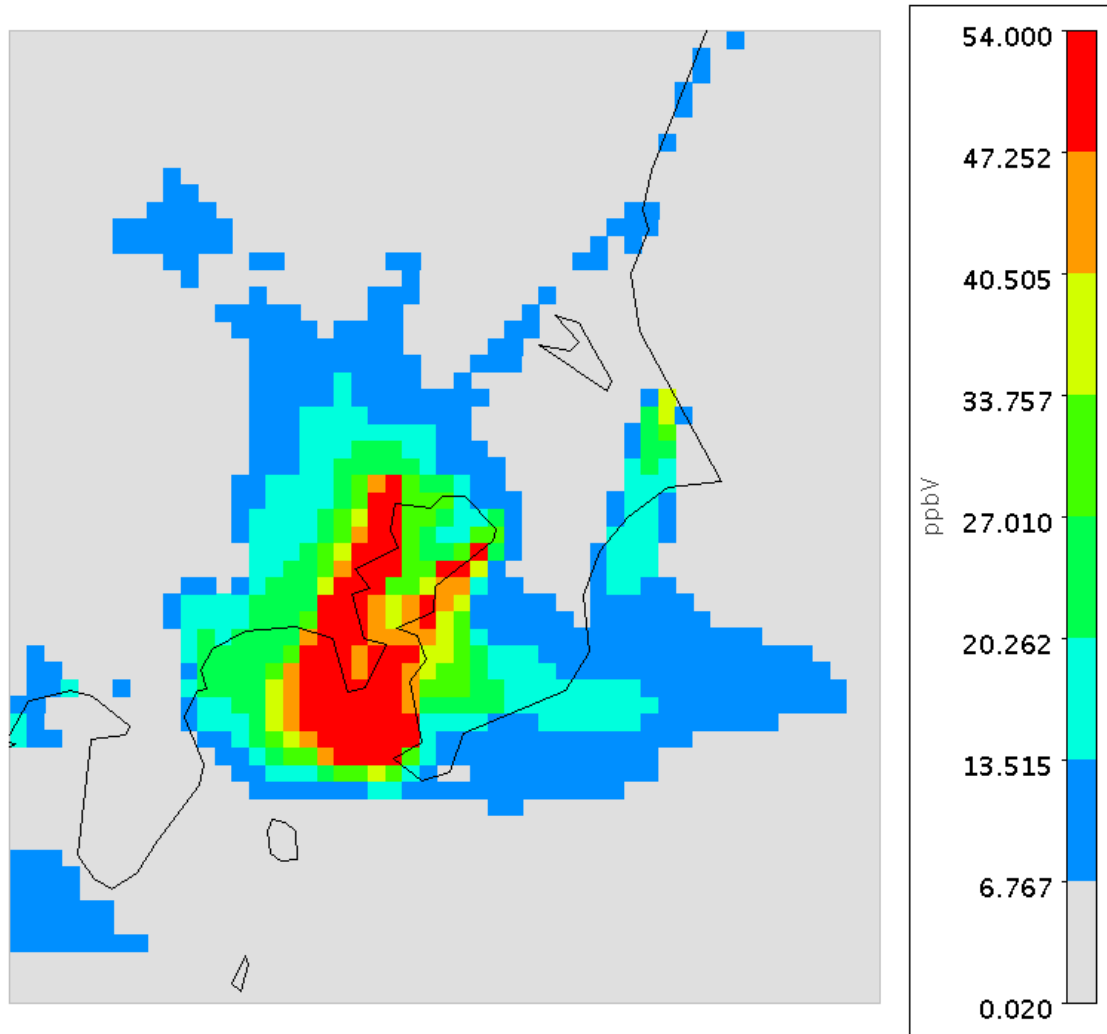


Fig.3.23 NOx concentration for base scenario, 7/30 8:00

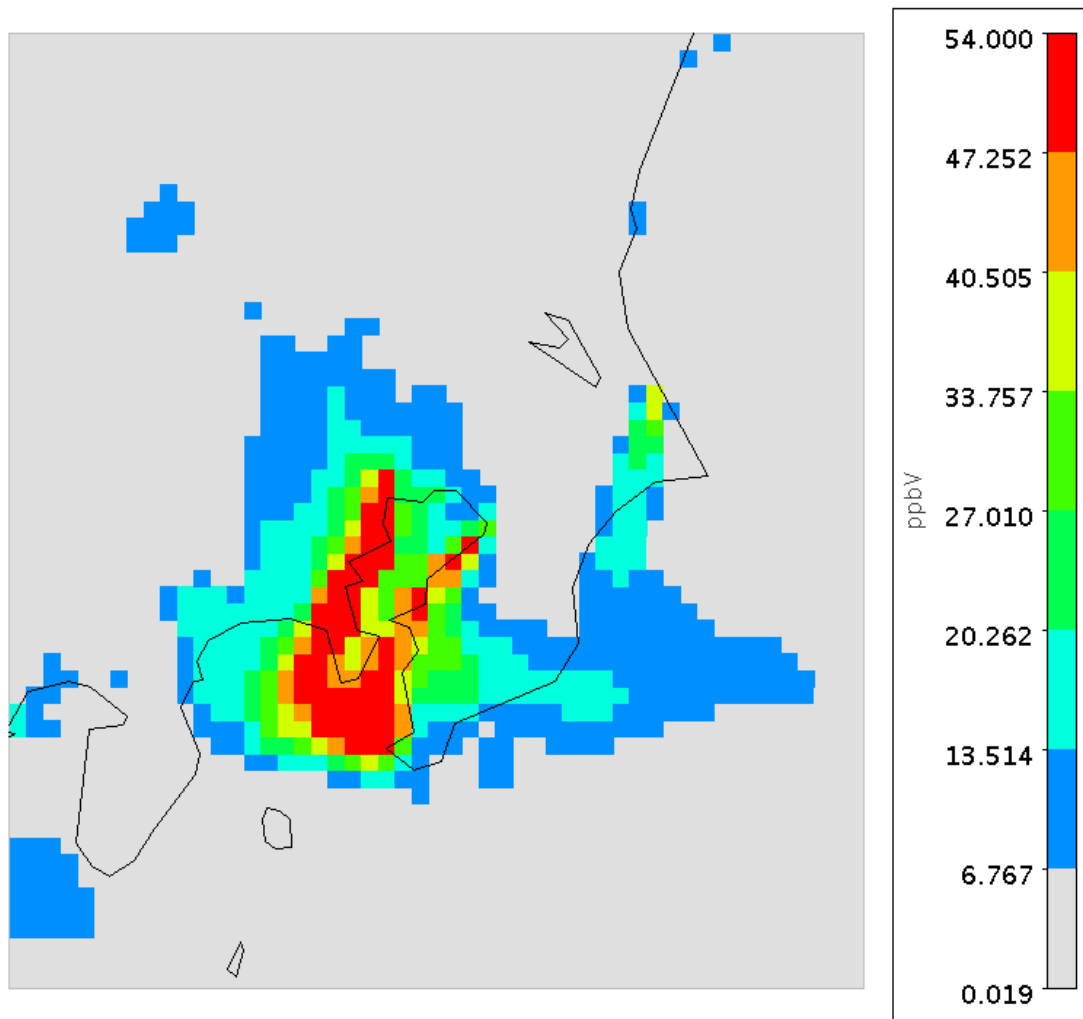


Fig.3.24 NOx concentration for hybrid 2 scenario, 7/30 8:00

Fig.3.25 shows the average NO<sub>x</sub> concentration change for the calculation period. It shows that the ozone increase area is in accordance with the NO<sub>x</sub> concentration decrease area, proving the NO<sub>x</sub> titration contributes a lot to the ozone concentration increase.

Here comes to the conclusion that the strange increase on sea surface is because of the wind transport of NO<sub>x</sub> from urban area to sea surface. With the reduction of NO<sub>x</sub> emission, sea surface NO<sub>x</sub> concentration decreases meanwhile, then the decrease of NO<sub>x</sub> titration caused the ozone increase.

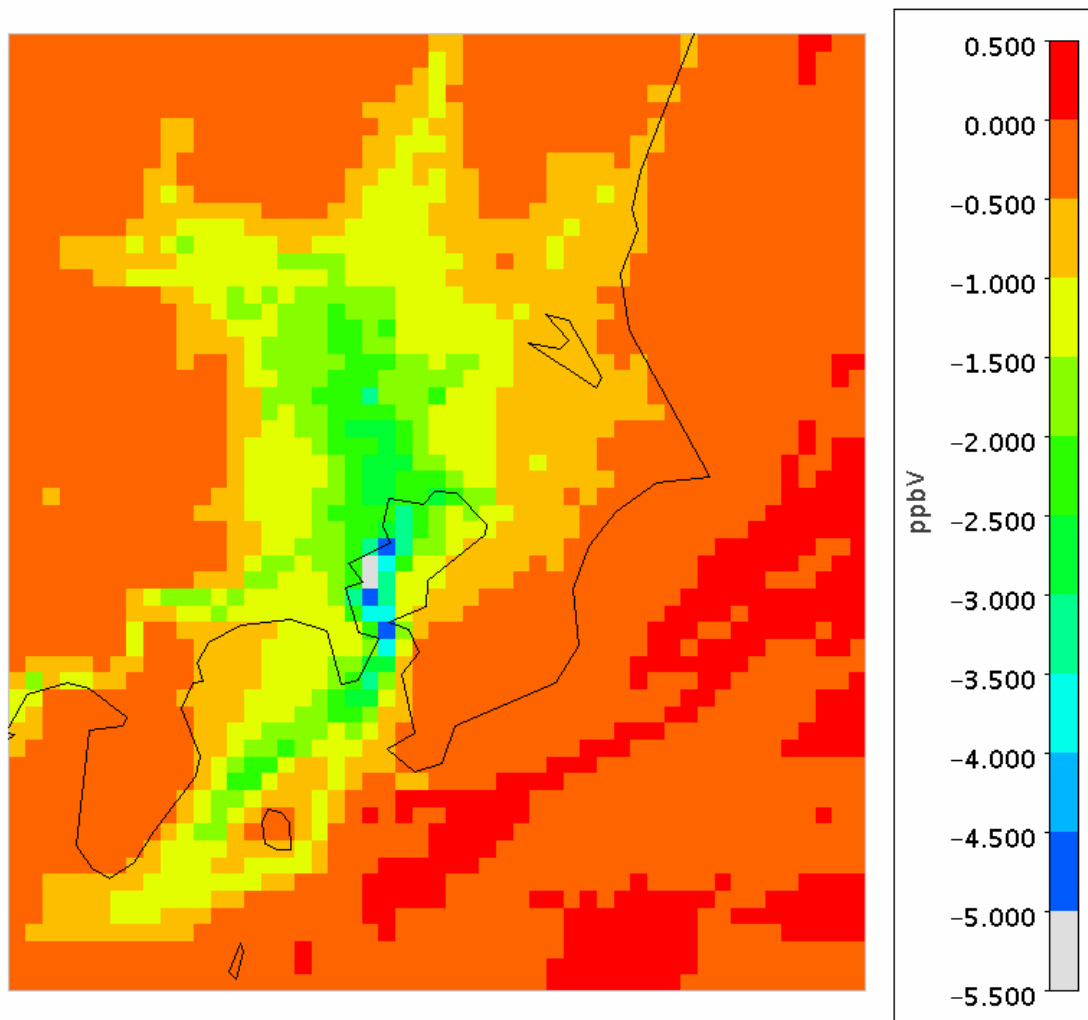


Fig.3.25 Average NO<sub>x</sub> concentration change for calculation period

### 3.3 Mortality estimation

The ozone associated mortality estimation can be generally concluded for two types, long-term exposure and short-term exposure [21]. For long-term estimation, the accumulate ozone exposure of a threshold of certain concentration is most focused [22] [23]. However, this simulation is just conducted for two weeks' calculation, and most of high ozone pollution cases appear in summer season, the short-term exposure of ozone is estimated. The key factor of short-term ozone mortality estimation is maximum 8-hour mean concentration. 8-hour mean for a certain hour is the mean of the hourly average concentration for that hour and preceding 7 hours.

Based on the calculation result, premature mortality change associated with ozone can be estimated by following equation [25]

$$y = y_0 \cdot (1 - e^{-\beta \cdot \Delta x}) \cdot P$$

where

$y$ : Premature mortality change

$y_0$ : Baseline incidence rate per unit population

$\beta$ : Ozone concentration–response coefficient

$$\beta = \frac{\ln RR}{\Delta[O_3]_{RR}}$$

$RR$ : Relative risk for ozone, 1.003 suggested by WHO [26]

$\Delta[O_3]_{RR}$ :  $10 \mu\text{g}/\text{m}^3$

$\Delta x$ : Concentration change of maximum 8-hour ozone mean concentration

$P$ : Population

Table 3.1 shows the 8-hour maximum concentration change calculated by CMAQ model. With higher NOx reduction rate, the ozone concentration changes are higher as well

Table 3.1 8-hour maximum concentration change for capital area

$\Delta O_3/ppbv$	Ibaraki	Tochigi	Gunma	Saitama	Chiba	Tokyo	Kanagawa
hybrid 1	0.027	0.029	0.024	0.037	0.03	0.039	0.028
hybrid 2	0.849	0.521	-0.407	1.326	0.307	1.207	0.985

Table 3.2 show the mortality change rate for capital areas of seven prefectures in the Kanto area. The mortality changes range from minimum -0.024% to the maximum 0.079% for hybrid 2 scenario.

Table 3.2 Mortality change rate (%) for capital area

Scenario	hybrid 1	hybrid 2
Mito	0.0016	0.0509
Utsunomiya	0.0017	0.0312
Maebashi	0.0014	-0.0244
Saitama	0.0022	0.0794
Chiba	0.0018	0.0184
Shinjuku	0.0023	0.0723
Yokohama	0.0017	0.0590

Table 3.3 shows the total Japanese mortality of 2013, from National Institute of Population and Social Security Research. High mortality increase are in accordance with high mortality number, means that the health effect for these high population density area is quite severe.

Table 3.3 Total mortality, 2013<sup>[27]</sup>

Prefecture	Total mortality
Ibaraki	30368
Tochigi	20591
Gunma	21661
Saitama	60264
Chiba	53603
Tokyo	110507
Kanagawa	72970

Introducing current diesel hybrid vehicle do not affect much. But with the development of technologies and NOx reduction ratio, the consequence becomes more severe. For example, the rate of mortality caused by traffic accidents is 0.32%, compared with the 0.07% mortality increase of ozone alone, the further effects on mortality cannot be ignored. Noticing that this is the rough calculation for only capital area of every area, the highest population density area, the effect of whole prefecture may be more serious.

## 4 Summary

### 4.1 Current Conclusion

The CMAQ model for predicting urban area ozone concentration is reliable with the high correlation coefficient. However, CMAQ model have the tendency to overestimated ozone concentration at night time for rural area.

The NO<sub>x</sub> emission reduction has contrast results on ozone concentration: increase in urban the area and decrease in the rural area.

For the short calculation period, the influence of wind is rather strong, longer period calculation is suggested for more precise calculation results.

Under current diesel hybrid technologies conditions, introducing diesel-hybrid vehicles do not affect atmosphere environment. With the improvement on battery and engine management, different counter measures should be enacted by analyzing specific VOC-NO<sub>x</sub>-ozone sensitivity. The introduction of hybrid vehicle sometimes can be harmful for ozone concentration and human health.

Mortality estimation shows that slight change in ozone concentration should be concerned for the high population density and influence of urban area.

## 4.2 Future plans

In this research, only CMAQ default boundary conditions are used. Other global emission inventories, such as HATP-2 and MOZART-4 are widely used as well. Same simulation may be done with different global emission inventories to evaluate their performances separately.

For winter season, because of the pollutant transportation from China and less solar radiation, the ozone concentration can be affected by these factors. Further simulations for winter season can be done to have a thorough view of ozone concentration change.

For the term of human health effect, PM<sub>2.5</sub> has a much higher relative risk value of 1.04 than ozone relative risk of 1.003. Different from ozone, the health effect of PM<sub>2.5</sub> is associated with its composition, which depends on both local anthropogenic emission and biogenic emission<sup>[28]</sup>. And most of all, the PM<sub>2.5</sub> calculation is not in good accordance with observed data, because the formation mechanisms of secondary organic carbon are not fully revealed. Further research can be done in this field.

## Acknowledgment

I would like to express all my gratitude to those who helped and supported me during the writing of this essay.

My deepest gratitude goes first to my supervisor, Professor Tonokura, for his consistent patience and rigorous instruction. From the proposal to the preparation, from the intermediate presentation to the final master thesis, his inspiring encouragement and detailed guidance help me through all the difficulties of two years master research. He taught me not only on this essay, but also the scientific methods to explore the unknowns systematically, which is of critical importance for further research. Without his help, this thesis could not have reached its present form.

Second, I would like to express my gratitude to Professor Tasaki, my co-research advisor. Although from different research field, his valuable suggestion still helps me arrange my thought of the whole research and benefits my final presentation. And I would like to thank all professors in the Department of Environment System, their lessons on variable fields build my knowledge fundament and broaden my eyes.

Special thanks to my laboratory mates, for sharing the progress, discussing the problems, and overcoming difficulties together. I am happy to get to know them.

At last, I really appreciate my beloved parents. I owe them too much. It was their understanding that make me study oversea alone, and their support without a complaint help me through all these years.

## Reference

- [1] Air pollution condition report for 2016 (2016 年度大気汚染の状況 環境省)  
<http://www.env.go.jp/air/osen/28taikiosen.pdf>
- [2] Proceedings The Empirical Kinetic Modeling Approach (ekma) Validation Workshop, US EPA, 1983
- [3] Jerrett, M., R.T. Burnett, C.A. Pope, K. Ito, G. Thurston, D. Krewski, Y.L. Shi, E. Calle, and M. Thun. 2009. Long-term ozone exposure and mortality. *N. Engl. J. Med.* 360(11):1085–95. doi:10.1056/NEJMoa0803894
- [4] Bell, M.L., F. Dominici, and J.M. Samet. 2005. A meta-analysis of time-series studies of ozone and mortality with comparison to the national morbidity, mortality, and air pollution study. *Epidemiology* 16(4):436–45. doi:10.1097/01.ede.0000165817.40152.85
- [5] Ito, K., S. F. De Leon, and L. Morton. 2005. Associations between ozone and daily mortality: analysis and meta-analysis. *Epidemiology* 16(4):446–57. doi:10.2307/20486080
- [6] Kampa M, Castanas E (2008) Human health effects of air pollution. *Environ Pollut* 151:362–367
- [7] Fu JS, Dong X, Sensitivity and linearity analysis of ozone in East Asia: the effects of domestic emission and intercontinental transport, *J Air Waste Manag Assoc.* 2012 Sep;62(9):1102-14.
- [8] Shiri A., Denise L.M., Global crop yield reductions due to surface ozone exposure: 2. Year 2030 potential crop production losses and economic damage under two scenarios of O<sub>3</sub> pollution, *Atmospheric Environment* Volume 45, Issue 13, April 2011, Pages 2297-2309
- [9] Ibrahim.A.R., The pollutant emissions from diesel-engine vehicles and exhaust aftertreatment systems, *Clean Techn Environ Policy* (2015) 17:15–27
- [10] Hiroyuki Y, Misawa K, Suzuki D, Tanaka K, Matsumoto J, Fujii M, Tanaka K (2011) Detailed analysis of diesel vehicle exhaust emissions: nitrogen

oxides, hydrocarbons and particulate size distributions. Proc Combust Inst 33:2895–2902

[11] Biswas S, Verma V, Schauer JJ, Sioutas C (2009) Chemical speciation of PM emissions from heavy-duty diesel vehicles equipped with diesel particulate filter (DPF) and selective catalytic reduction (SCR) retrofits. Atmos Environ 43: 1917–1925

[12] Pallavi Pant, Estimation of the contribution of road traffic emissions to particulate matter concentrations from field measurements: A review, Atmospheric Environment 77 (2013) 78-97

[13] Fujita, E.M., Campbell, D.E., Arnott, W.P., Chow, J.C., Zielinska, B., 2007. Evaluations of the chemical mass balance method for determining contributions of gasoline and diesel exhaust to ambient carbonaceous aerosols. Journal of Air and Waste Management Association 57, 721-740.

[14] Sydbom A, Blomberg A, Parnia S, Stenfors N, Sandstrom T, Dahlen SE (2001) Health effects of diesel exhaust emissions. Eur Respir 17:733–746

[15] Annual report of automobile vehicle fuel consumption(自動車燃料消費量統計)<http://www.mlit.go.jp/k-toukei/search/pdf/22/22201700a00000.pdf>

[16] Ministry of Environment, Efforts on saving atmospheric environment. <https://www.env.go.jp/council/07air-noise/y078-03/ref02/>参考資料 2 大気環境保全に関するこれまでの取組.pdf

[17] US EPA, <https://www.epa.gov/cmaq/cmaq-models-0>

[18] Japan Meteorological Agency [https://www.data.jma.go.jp/obd/stats/etrn/view/daily\\_2013\\_7\\_day](https://www.data.jma.go.jp/obd/stats/etrn/view/daily_2013_7_day)

[19] Mathur, Multiscale air quality simulation platform: Initial applications and performance for tropospheric ozone and particulate matter, J. Geophys. Res., 2005

[20] Morino, Yu & Chatani, Satoru & Hayami, Hiroshi & Sasaki, Kansuke & Mori, Yasuaki & Morikawa, Tazuko & Ohara, Toshimasa & Hasegawa, Shuichi & Kobayashi, Shinji. (2010). Inter-comparison of Chemical Transport Models and Evaluation of Model Performance for O3 and PM2.5 Prediction - Case

Study in the Kanto Area in Summer 2007. 大気環境学会誌. 212-226.  
10.11298/taiki.45.212.

[21] Salvi S, Blomberg A, Rudell B, et al. Acute inflammatory responses in the airways and peripheral blood after short-term exposure to diesel exhaust in healthy human volunteers. *Am J Respir Crit Care Med*. 1999; 159:702–709.

[22] Kloog, I., Ridgway, B., Koutrakis, P., Coull, B. A., & Schwartz, J. D. (2013). Long- and short-term exposure to PM<sub>2.5</sub> and mortality: using novel exposure models. *Epidemiology (Cambridge, Mass.)*, 24(4), 555-61.

[23] Crouse DL, Peters PA, van Donkelaar A, et al. Risk of nonaccidental and cardiovascular mortality in relation to long-term exposure to low concentrations of fine particulate matter: a Canadian National-Level Cohort Study. *Environ Health Perspect*. 2012; 120:708–714

[24] Knowlton, K., J.E. Rosenthal, C. Hogrefe, B. Lynn, S. Gaffin, R. Goldberg, C. Rosenzweig, K. Civerolo, J.Y. Ku, and P.L. Kinney. 2004. Assessing ozone-related health impacts under a changing climate. *Environ. Health Perspect*. 112(15):1557–1563. doi:10.2307/3435615

[25] Sun J, Fu JS, Estimation of future PM<sub>2.5</sub>- and ozone-related mortality over the continental United States in a changing climate: An application of high-resolution dynamical downscaling technique, *J Air Waste Manag Assoc*. 2015 May;65(5):611-23. doi: 10.1080/10962247.2015.1033068.

[26] Effects of air pollution on children's health and development. A review of the evidence. Copenhagen, WHO Regional Office for Europe, 2005

[27] National Institute of Population and Social Security Research: Japanese Mortality Database <http://www.ipss.go.jp/p-toukei/JMD/index.asp>

[28] Jacobson, M.Z. 2012. *Air Pollution and Global Warming: History, Science and Solutions*, 2nd ed. New York, NY: Cambridge University Press, New York.